

A review on the heterostructure nanomaterials for supercapacitor application

Sanjit Saha^{a,b}, Pranab Samanta^a, Naresh Chandra Murmu^a, Tapas Kuila^{a,*}

^a Surface Engineering & Tribology Division, CSIR-Central Mechanical Engineering Research Institute, Durgapur 713209, India

^b Academy of Scientific and Innovative Research (AcSIR), CSIR-CMERI Campus, Durgapur 713209, India



ARTICLE INFO

Article history:

Received 23 January 2018

Received in revised form 16 March 2018

Accepted 16 March 2018

Available online 23 March 2018

Keywords:

Heterostructure

Hybridization

Supercapacitor

Carbonaceous materials

Redox materials

Doping

ABSTRACT

The typical physical and chemical properties lead the nanomaterials to breakthrough in the field of energy storage especially, supercapacitor applications. The optimization of electrical conductivity, structural flexibility, band gap and charge carrier mobility are the key point to solve the issues in the electrochemical charge storage mechanism of supercapacitor. The semiconducting heterostructured nanomaterials are the best choice to store energy by near-surface ion adsorption along with additional contribution from fast reversible faradic reactions. The creation of active sites and defects in the grain boundary of the heterostructure materials results in multiple redox activity, superior ionic conductivity and short diffusion path. Therefore, sufficient researches enrooted to the doped and nano heterostructure electrode materials needs to be performed in order to exploit the high power and energy storage applications. This article reviews current trends in the synthesis of heterostructure electrode through hybridization of different electrochemical double layer capacitance (EDLC) and pseudocapacitive materials. This article also emphasize on the effect of doping on the electrode possessing both EDLC as well as the pseudocapacitance. In addition, the advantages of superlattice structure for the superior electrochemical properties are also discussed.

© 2018 Elsevier Ltd. All rights reserved.

Contents

1. Introduction	182
2. Heterostructure nanomaterials	182
2.1. Heterostructure electrode formed by hybridization of different pseudocapacitive materials	182
2.1.1. Heterostructure electrode of binary metal oxides	183
2.1.2. Heterostructure electrode of ternary metal oxides	185
2.1.3. Heterostructure electrode of polymer and metal oxides	186
2.2. Heterostructure electrode formed by hybridization of EDLC and pseudocapacitive materials	186
2.2.1. Hybridization of EDLC and metal oxide/hydroxide	187
2.2.2. Hybridization of EDLC and conducting polymers	190
2.3. Doping of the supercapacitor electrode materials	192
2.3.1. Doping of the EDLC electrode materials	192
2.3.2. Doping of the redox materials	195
2.4. Superlattice electrode materials	197
3. Conclusions and outlook	198
Acknowledgements	199
References	199

* Corresponding author.

E-mail address: t_kuila@cmeri.res.in (T. Kuila).

1. Introduction

The inadequate storage of fossil fuels and global warming are the major energy security concerns, which prompt major concentration to expand and develop the renewable energy technologies [1–3]. Indeed, the hurried rise of energy productions from renewable sources like solar and wind, forced to develop new generation energy storage system as because the renewable sources cannot produce energy on demand [1–5]. However, the effective and efficient utility of the entire energy and power by the storing system are still the major challenges of the current research. Especially, the present battery systems face difficulties during the peak power demands [1–5]. Supercapacitor is the most prospective energy storage devices in this regard. Several research works were carried out to enhance the energy storage and deliver applications of supercapacitor through last decade [6–9]. The typical physical and chemical properties lead the nanomaterials to several breakthroughs in the fundamental as well as applied scientific areas such as energy storage or supercapacitor applications. Generally, two kinds of materials are used as supercapacitor electrode [5–9]. One kind of materials store charges through surface adsorption called electrochemical double layer capacitance (EDLC). Carbonaceous materials like graphene, reduced graphene oxide (rGO), carbon nano tube (CNT) and activated carbons are used as the EDLC electrode. On the other hand, materials store charges by faradic redox reaction called pseudocapacitive materials. Different metal oxide, hydroxide and conducting polymers are used as the pseudocapacitive electrodes.

However, such type materials face difficulties during practical applications. The optimization of electrical conductivity, structural flexibility, band gap and charge carrier mobility are the key point to solve the issues in the electrochemical charge storage mechanism of supercapacitor [10–15]. Fabrication of nano heterostructures is the appropriate solution to store energy by near-surface ion adsorption along with additional contribution from fast reversible faradic reactions. The creation of active sites and defects in the grain boundary of the heterostructure materials results in multiple redox activity, superior ionic conductivity and short diffusion path. Furthermore; doping is elementary to control the electrical properties of poorly conductive materials through fine adjustment of highest occupied molecular orbital (HOMO) and lowest occupied molecular orbital (LUMO) energy levels of host and guest in doped electrode materials providing the desirable properties of high power density, fast charge/discharge process and long life span [16–18]. Therefore, sufficient researches enrooted to the doped and nano heterostructure electrode materials needs to be performed in order to exploit the high power and energy storage applications [16–18]. Recently, different types of multimetal oxide, core shell and spinal structures were developed through different chemical route, simple hydrothermal treatment and high temperature calcinations process. The creation of defects, vacancies and active sites in between the grain boundary of the heterostructure influence the ionic conductivity and diffusion path of the electrolyte through the electrode materials [21,22]. The size and the structural orientation of the particles are possible by controlling the presence of different phase or grain in a single system. The surface area and the porosity of the multimetal oxide also increase significantly as compared to the single metal oxide as the electrode materials. In addition, hybridization of EDLC and pseudocapacitive materials is another way to improve the electrochemical properties of the materials [19,20]. Nano scale hybridization of EDLC and pseudocapacitive electrode materials of different dimensionalities enlarge the surface area and enhance the active electrochemical sites. On the other hand, band gap of the poorly electrically conductive

electrode materials is modified through external doping. The optimized doping significantly enhances the tunneling probability and mobility of the charge carrier rises which in turn increase the quick charge discharge and stability of the electrode even in the high current density.

This article reviews current trends in the synthesis of heterostructure materials and the effect of external doping on the electrochemical double layer capacitance (EDLC) as well as the pseudocapacitance. Based on the researches carried out till date, the study on the advantages of the heterostructure and doping of the electrode materials can be divide in to three categories: (i) heterostructure electrode formed by hybridization of different pseudocapacitive materials, (ii) heterostructure electrode formed by hybridization of EDLC and pseudocapacitive materials, (iii) doping of the supercapacitor electrode materials, and (iv) superlattice electrode materials. The carbonaceous materials such as reduced GO (rGO), graphene, CNT and activated carbon are used as the EDLC electrode materials. On the other hand, the metal oxide, hydroxide and polymers are used as the redox or pseudocapacitive electrode materials. The hybridization of different EDLC and pseudocapacitive materials results in superior heterostructure with high energy and power density. The raise in the available free charge carrier of the EDLC materials is achievable through doping. On the other hand, significant increase in energy and power density of the composite materials is observed by positive or negative doping. Superlattice is the kind of heterostructure where layers of different materials can be arranged periodically in nanometer dimension. The superior incorporation of different active materials in superlattice provides high electrochemical properties.

2. Heterostructure nanomaterials

Heterostructure is formed with more than one component. Designing of heterostructure electrode is advantageous as because the improvement of intrinsic properties of each component is achieved in terms of superior electrical conductivity, rapid ionic transport, cycle stability and greater electrochemical reversibility. The motto of the present research is to improve the energy density in supercapacitors, without affecting the power density. Transition-metal oxides and conducting polymers are popular electrode materials in terms of high energy density. On the other hand, carbonaceous materials provide rapid charging-discharging (CD) profile or high power delivery capacity. Hybridization of different metal oxide/hydroxide in 1–3 D heterostructure form provides efficient electron/ion transport pathway, electrochemical active sites and different oxidation-reduction potential. In addition, hybridization of carbonaceous materials with high-energy materials (metal oxides or conductive polymers) can lead to electrical conductivity and high electrochemically accessible area. Heterostructure is also formed by introducing heteroatom within the crystal of EDLC or pseudocapacitive type of materials. Doping of metal oxide provides additional electron enhancing the electrical conductivity and generates defects, which acts as electrochemical active sites. On the other hand, doping can open small band gap in carbonaceous materials providing semiconducting nature and redox activity.

2.1. Heterostructure electrode formed by hybridization of different pseudocapacitive materials

Heterostructure multimetal oxides show various crystalline structure and widely used as supercapacitor electrodes. Multimetal oxides of transition metals are synthesized to accumulate the superior electrochemical properties of two or more metal oxides.

2.1.1. Heterostructure electrode of binary metal oxides

Heterostructured binary metal oxides were synthesized in different techniques like hydrothermal, microwave assisted template, sol-gel and electro deposition method. It is possible to achieve different architecture of heterostructure metal oxides by controlling the reaction temperature or time. The electrochemical performances also varied significantly with changing the morphology of the multi metal oxide electrodes. NiCo_2O_4 was synthesized through hydrothermal method with different temperature and time [23–27]. The synergistic advantages from two different metal ions provide superior electrochemical properties as compared to the bare metal oxides [23–27]. Furthermore, the electrical conductivity increased due to the formation of heterostructure of spinal binary oxides. The enhanced charge storage capacity of NiCo_2O_4 was ascribed to the two-redox reaction originated from the two different active sites in an alkaline electrolyte [23–27]. The rate capability of the metal oxides is comparatively low due to the faradic redox charge transfer. However, the free charge carriers were produced due to the creation of defects during the growth of heterostructure multi-metal oxides. Defect induced mechanism are helpful for achieving superior electrochemical charge storage properties even at the high scan rate or large current density. On the other hand, defect induced free charge carriers improved the electrical conductivity of the electrode materials. As a result, the solution resistance at the electrode-electrolyte interface decreased due to the facile electrical conductivity. Low solution resistance also contributed to improve the charge storage capacity of the heterostructure multi-metal oxides. The pH of the reaction medium controlled the

morphology of NiCo_2O_4 . Wang et al. showed the formation of three different structures (nanorod-to-straw bundles-to-urchin spheres) of NiCo_2O_4 by varying the pH value during the hydrothermal synthesis (Fig. 1(a–c)) [23]. Fig. 1(d & e) shows the CV and CD of NiCo_2O_4 at different scan rate and current density, respectively. The surface area as well as electron accessibility of NiCo_2O_4 varied with different morphology and a high specific capacitance of 1650 F g^{-1} was achieved at 1 A g^{-1} current density. Although the origin of charge storage in NiCo_2O_4 is diffusion controlled redox reaction, the rate capability remained 81.7% for the urchin-like NiCo_2O_4 nano structure [23]. The high retention was ascribed to the effective utilization of active sites at the outside surface of urchin-like NiCo_2O_4 .

Iron, molybdenum and cobalt based multimetal oxides showed promising supercapacitor properties due to their unique morphology and redox activity [28–32]. Zhang et al. reported the partial conversion of current collector into nickel copper oxide electrode materials. This strategy is advantageous as because the difficulty associated with the poor interfacial contact between electrode materials and current collector was resolved as well as the supercapacitor weight was minimized.

Fig. 2a shows the FE-SEM image of pure Cu foam. Two consecutive oxidation steps were used to modify the current collector with electrode material. The FE-SEM images of the modified electrode are shown in Fig. 2b (after oxidization) and 2c (after hydrothermal reaction). It was found from the XPS analysis that nickel (II) was present along with Cu^{2+} , which established the formation of Cu/Ni binary oxide. The composition of Cu and NiO heterostructure was further confirmed by elemental mapping from

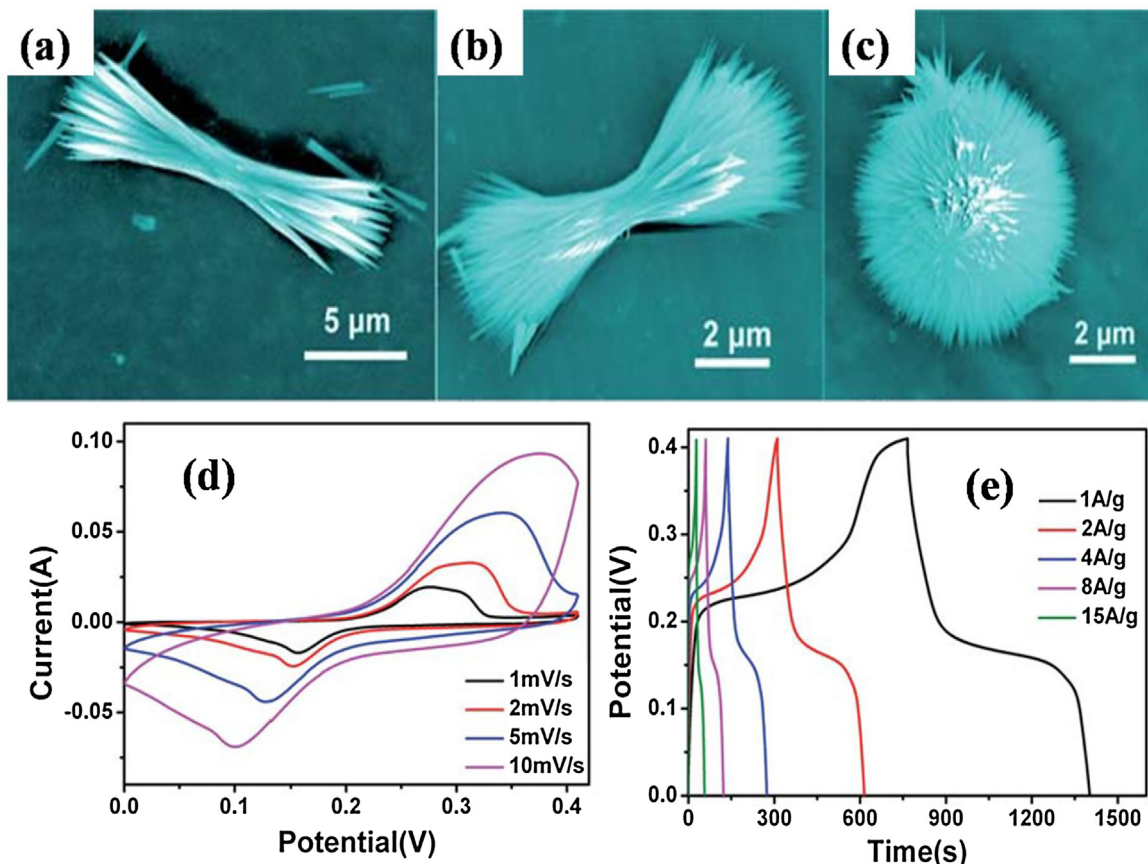


Fig. 1. (a–c) SEM images of the NiCo_2O_4 products obtained under a hydrothermal process with pH values of 5.5, 6.1 and 6.8, respectively. Electrochemical properties of the electrode materials measured using a three-electrode system in 3.0 mol L^{-1} KOH aqueous electrolyte: (d) CV at different scan rates for sea-urchin electrode; (e) comparative CV curves recorded at a scan rate of 2 mV s^{-1} for the two different electrodes. Reproduced from Ref. [23] with permission from Royal Society of Chemistry.

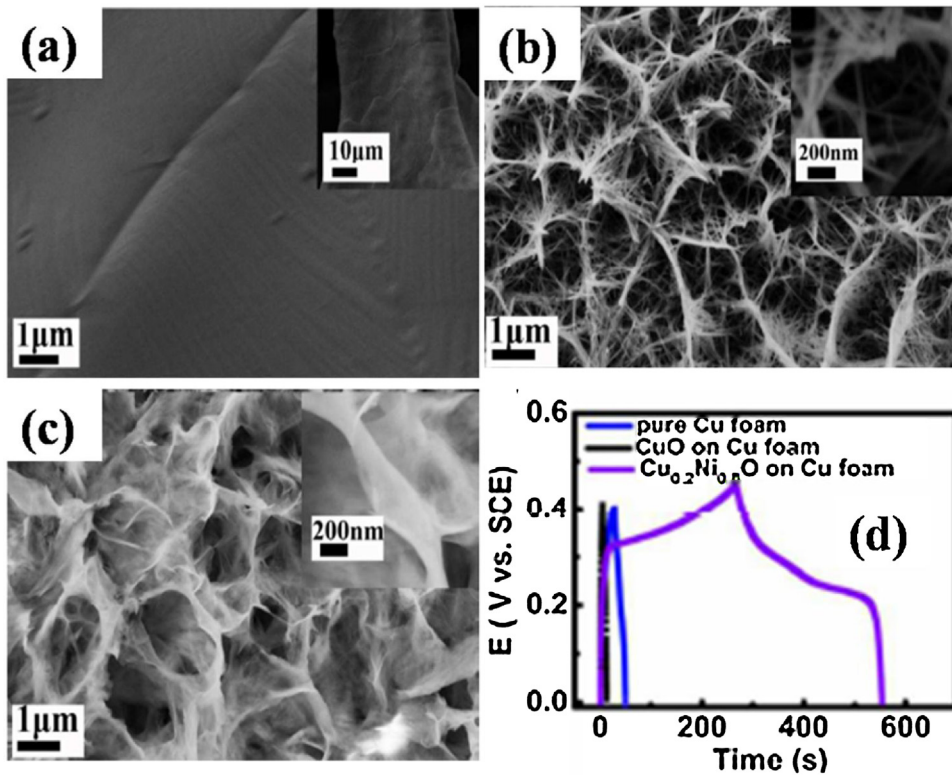


Fig. 2. FE-SEM images of (a) original copper foam; (b) after the first processing step: oxidization; (c) after the second processing step: hydrothermal reaction, and (d) GCD curves at 5 mA cm^{-2} of pure Cu foam, CuO on Cu foam and $\text{Cu}_{0.2}\text{Ni}_{0.8}\text{O}$ on Cu foam. Reproduced from Ref. [31] with permission from American Chemical Society.

scanning transmission electron microscopy (STEM). Furthermore, superior charge transfer was achieved without hampering the mechanical properties of the metal current collector. The comparison of the supercapacitive properties of pure Cu foam and modified electrodes is shown in Fig. 2d. Finally, $\text{Cu}_{0.2}\text{Ni}_{0.8}\text{O}$ showed high areal capacitance of 3.13 F cm^{-2} at a current density of 1 A g^{-1} [31]. $\text{MnO}_2/\text{NiO}@\text{Ni}$ heterostructure electrode was prepared through simple one step hydrothermal reaction [33]. The active material was directly grown on the Ni-foam where Ni was oxidized to NiO and KMnO_4 was reduced to MnO_2 [33]. Ultrathin MnO_2/NiO nano flakes showed a reversible and fast redox reaction

as the result of available short diffusion path for electrolyte ions. In addition, in-situ electrode preparation by direct growth of NiO on the Ni-foam was advantageous as the use of any non-conductive polymer binder can be avoided. The gravimetric capacitance of the MnO_2/NiO electrode was measured as 980 F g^{-1} at 10 mV s^{-1} scan rate [33]. The morphology of the heterostructure metal-based electrode was superior in comparison to the individual metal oxide. The available pores in the multimetal oxides were larger than the bare metal oxides owing to the existence of different crystalline structure. This kind of structural features accelerated the diffusion of the electrolyte ions through the electrode

Table 1
Comparison of the supercapacitor properties of different multimetal oxides.

Electrode materials	Electrolyte	Potential window (V)	Specific capacitance (F g^{-1})	Current density (A g^{-1})	Retention of specific capacitance	References
NiCo_2O_4	3 M KOH	0 to 0.4	1650	1	~81% (15 A g^{-1})	[23]
NiCo_2O_4	2 M KOH	0 to 0.65	1.55 F cm^{-2}	2 mA cm^{-2}	~74% (40 mA cm^{-2})	[25]
NiCo_2O_4	6 M KOH	-0.1 to 0.4	401	1	~75% (8 A g^{-1})	[26]
NiCo_2O_4		-0.05 to 0.45	743	1	~78.6% (40 A g^{-1})	[27]
CoMoO_4	2 M KOH	-0.1 to 0.7	1.26 F cm^{-2}	4 mA cm^{-2}	~62% (32 mA cm^{-2})	[29]
$\text{CoMoO}_4\cdot0.9\text{H}_2\text{O}$	-	-0.2 to 0.5	326	5 mA cm^{-2}	~68% (50 mA cm^{-2})	[30]
$\text{Cu}_{0.2}\text{Ni}_{0.8}\text{O}$	KOH/PVA	0 to 0.5	3.13 F cm^{-2}	1	~94% (4 A g^{-1})	[31]
Ni-Co binary oxides	-	0 to 0.6	750	1	~66% (10 A g^{-1})	[32]
Mn-Ni-Co ternary oxide	6 M KOH	0 to 0.5	638	1	~63% (20 A g^{-1})	[34]
$\text{NiCo}_2\text{O}_4@\text{CoMoO}_4$	2 M KOH	-0.2 to 0.7	14.67 F cm^{-2}	10 mA cm^{-2}	~56.5% (60 mA cm^{-2})	[35]
$\text{Cu}_2\text{O}/\text{CuMoO}_4$	6 M KOH	0 to 0.6	4264	1	~73% (10 A g^{-1})	[36]
$\text{NiCo}_2\text{O}_4@\text{NiO}$	PVA/KOH	-0.9 to 0.9	1792	5 mA cm^{-2}	~76% (40 mA cm^{-2})	[38]
$\text{NiCo}_2\text{O}_4@\text{MnO}_2$	1 M NaOH	0 to 0.6	2.244 F cm^{-2}	2 mA cm^{-2}	~55% (50 mA cm^{-2})	[39]
Nickel-Cobalt Phosphate 2D Nanosheets	3 M KOH	0 to 0.6	1132.5	1	~63% (10 A g^{-1})	[40]
$\text{Co}_3\text{O}_4/\text{Co(OH)}_2$	3 M KOH	0 to 0.4	1164	1.2	~41% (15 A g^{-1})	[41]
Fe-Ni-Co oxide	1 M KOH	-0.5 to 0.5	867	3	~18% (10 A g^{-1})	[42]
Zn-Ni-Co ternary oxide	6 M KOH	0 to 0.5	2481.8	1	~91.9% (5 A g^{-1})	[43]
Ni-Co oxides/hydroxides	2 M KOH	-0.05 to 0.45	1884	3	~77.7% (30 A g^{-1})	[44]

materials. In addition, the presence of available redox active sites in heterostructure materials contributed high specific capacitance. The supercapacitor performances of the metal-based heterostructure electrodes are summarized in Table 1. It was found that the KOH-based electrolyte was used to analyze the supercapacitor properties of the multimetal oxides. The retention of the specific capacitance of the multimetal oxides was high even at very high scan rate or current density. About 70% retention of the specific capacitance of multimetal oxides was observed even with the 10 folds increase in the current density or scan rate.

2.1.2. Heterostructure electrode of ternary metal oxides

Ternary metal oxide nanomaterials show facile electrochemical performances due to the higher specific surface area and multiple redox activity [34–48]. Several synthesis processes like sol-gel, microwave, electrodeposition, hydrothermal, etc. were used to prepare the ternary metal oxide heterostructure. Nickel and cobalt based ternary oxides are most commonly used heterostructure electrode materials [35,37–39]. Electrochemical properties of NiCo_2O_4 were improved by hybridization with other metal/metal oxide through the formation of core-shell structure [35,37–39]. Surface area of the electrode materials was highly improved by the formation of core-shell structure [35,37,38]. Abrupt increase in energy density was recorded through hybridization of two pseudocapacitive elements. Electrical conductivity and the redox active site of the electrode material also increased due to the formation of core-shell heterostructure [35,37–39]. Furthermore, the space in between the core and shell provided high electron/ion diffusion for faradic reaction.

Xu et al. prepared NiCo_2O_4 on the nickel foam through hydrothermal reaction. NiCo_2O_4 was further modified to $\text{NiCo}_2\text{O}_4@\text{MnO}_2$ core-shell by electrodeposition technique (Fig. 3a) [39]. The current response was remarkably increased for $\text{NiCo}_2\text{O}_4@\text{MnO}_2$ as compared to the bare NiCo_2O_4 (Fig. 3b). The CD of NiCo_2O_4 and $\text{NiCo}_2\text{O}_4@\text{MnO}_2$ was compared at 2 mA cm^{-2} current density (Fig. 3c).

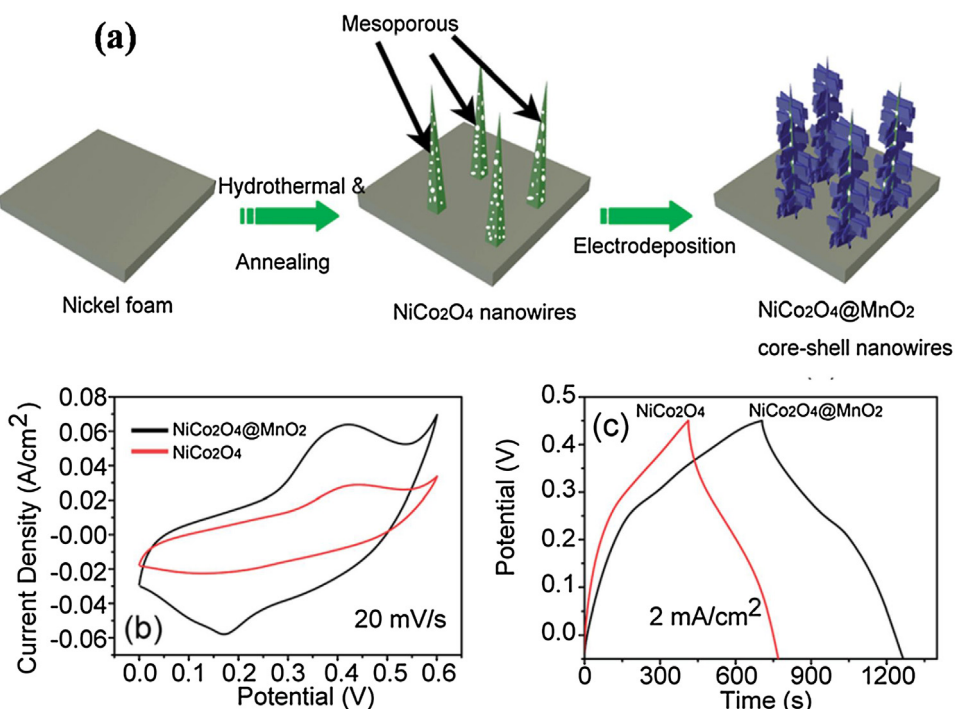


Fig. 3. (a) Schematic of the fabrication process for hierarchical mesoporous $\text{NiCo}_2\text{O}_4@\text{MnO}_2$ core–shell nanowire arrays on nickel foam, (b) CV curves of the hierarchical mesoporous $\text{NiCo}_2\text{O}_4@\text{MnO}_2$ core–shell nanowires, and (c) A comparison of the CD curves of as-synthesized electrode materials at a current density of 2 mA cm^{-2} . (Reproduced from Ref. [39] with permission from Royal Society of Chemistry).

2.224 F cm^{-2} for NiCo_2O_4 and $\text{NiCo}_2\text{O}_4@\text{MnO}_2$, respectively. The enhanced performance of the core–shell heterostructure was attributed to the unique architecture of the mesoporous $\text{NiCo}_2\text{O}_4@\text{MnO}_2$. The direct growth of NiCo_2O_4 on to the nickel foam provides electron “superhighways” for charge transfer and storage. Furthermore, the conducting NiCo_2O_4 overcomes the poor conductivity of MnO_2 .

Xu et al. described the core–shell heterostructure as the ion reservoir for diffusion controlled reaction where the transport resistance was minimized successfully. In addition, the core–shell electrode was able to perform at high current density due to the facile intercalation/deintercalation of ions originated from the mesoporous heterostructure. Core–shell nano-wire/nano-tube of ternary metal oxides also showed potential applications as supercapacitor electrodes [34,37,38]. In general, nano-wire provides high active surface area, rapid electron and ion transfer and superior structure stability.

Li et al. showed superior electrochemical performance of spinel manganese-nickel-cobalt ternary oxide nano-wire originated from the facile electrolyte diffusion through large surface area and the open geometry among the nano-wires [34]. The utilization of major portion of the redox active site is possible when the core–shell nano-wire was formed. In addition, the nano-wire heterostructure remained stable during charge discharge process and increased the life stability of the supercapacitor. Ultrathin and small particle size of the ternary metal-based heterostructure electrode contributed to the superior charge storage properties. The electrons or charge carriers were not confined within the interlayer of the different phase of the ternary metal alloys. In addition, ultrahigh specific surface area, and availability of abundant pores enhanced the diffusion controlled charge storage capacity. Low charge transfer resistance of the ternary metal oxides provided fast redox mechanism. As a result, the ternary metal alloys showed comparatively better supercapacitor properties in comparison to the binary metal heterostructure (Table 1).

2.1.3. Heterostructure electrode of polymer and metal oxides

Conducting polymers can store charges through the faradic reaction. Ions are transferred to the polymer backbone during oxidation and ions are released during the reduction process. The conducting polymers like polyaniline (PANI), polypyrrole (PPy) and their corresponding derivatives were widely used in energy storage applications [48–55]. These polymers show superior electrochemical properties like wide potential window and high rate of charge discharge process. However, poor stability, mechanical degradation, and high resistance are the main drawbacks of conducting polymers for supercapacitor applications [48–55]. Developing heterostructure electrode materials with conducting polymers and different metal oxides was a major step to overcome these limitations. Incorporation of metal oxide and conducting polymers are advantageous due to the availability of multiple redox mechanism. Enhanced current response in CV and longer discharging was achieved with integration of metal oxide in PANI [49,51,54].

Liu et al. showed that discharging time of PANI/MnO₂ heterostructure was much better than that of the bare PANI electrode (Fig. 4a) [54]. Bare PANI electrode discharged within 800 s while the PANI/MnO₂ heterostructure took 1100 s to discharge at 0.5 A g⁻¹ current density. The specific capacitance of pure PANI and PANI/MnO₂ was calculated as 662 and 810 F g⁻¹, respectively. In addition the effect of MnO₂ on the electrical/electrochemical properties of PANI electrode was investigated through Nyquist analysis (Fig. 4b) [54].

The charge transfer resistance of the bare PANI electrode was highly improved through MnO₂ incorporation. On the other hand, the Nyquist characteristic shifted towards more ideal capacitance when formed heterostructure with MnO₂. PANI had rod like architecture and remained intact after incorporation of MnO₂ (Fig. 5a & b) [54]. The cross-linking of the nano rods formed three-dimensional networks for facile electron transfer between the electrolyte and electrode materials. MnO₂ was uniformly deposited on the PANI. The formation of heterostructure increased the surface area, which in turn provides higher electrolyte accessibility to the active sites. There are a few reports to improve the electrical conductivity through the hybridization of multi metal oxide with PANI or by introducing metal nano particles with metal oxide/PANI composite [49,55]. The presence of multimetal oxide provided extra active sites along with enlarged surface area while the metal nano particles enhanced the electrical conductivity of the electrode. Charge delocalization was created due to the presence of NiCo₂O₄ on the backbone of PANI. Xu et al. studied the effect of different wt% of NiCo₂O₄ incorporation on PANI. Short ion diffusion

path of Ni²⁺ and Co³⁺ facilitated the electron transfers at the interface of electrode-electrolyte [55]. Furthermore, the formation of heterostructure created rough surface, which was advantageous for charge transfer between electrode materials and electrolyte. It was reflected from the EIS analysis that the NiCo₂O₄ incorporation effectively reduced the charge transfer resistance of the electrode due to which the overall electrochemical properties was improved. The increased slope of EIS plot at the lower frequency region suggested the presence of NiCo₂O₄ within PANI leads to the ideal capacitance behavior. The supercapacitor properties of the polymer/metal oxides electrode materials were compared in Table 2. The electrochemical performance was analyzed by using different acidic and basic electrolyte solution. However, the supercapacitor properties of the polymer/metal oxides were comparatively lower than the binary or ternary metal alloys. In addition, the rate capability of the polymer/metal oxides were lowers in comparison to the binary or ternary metal alloys. The retention of specific capacitance was lower at higher scan rate or current density.

2.2. Heterostructure electrode formed by hybridization of EDLC and pseudocapacitive materials

Electrochemical performance can be highly modified by combining the advantages of both redox reactions and ion adsorption to store electrical energy in the supercapacitor electrode [56–65]. This kind of modification led the supercapacitor to replace batteries as well as in harvesting applications when high power is required. Generally, the EDLC materials show fast charge/discharge rate, wide potential window, long stability, high electrical conductivity and high surface area. On the other hand, the pseudocapacitive materials have huge charge storage capacity due to the fast redox reactions (battery-like behavior). However, the charge discharge rate, stability and rate capability of pseudocapacitor materials is lower as compared to the EDLC electrode. Hybridization of EDLC and pseudocapacitive materials overcome the individual limitations and provides high energy and power densities along with fast charge discharge, high rate capability, long stability, etc. carbon materials are most prospective EDLC materials for supercapacitor applications [66–80]. Advantages of carbonaceous materials are large surface area, high electronic conductivity and chemical stability. Different types of carbonaceous materials like porous carbon, activated carbon, carbon nano tube (CNT) and graphene or reduced graphene oxide (rGO) were utilized for supercapacitor applications [71–80]. Carbonaceous materials exhibited small pore size and large

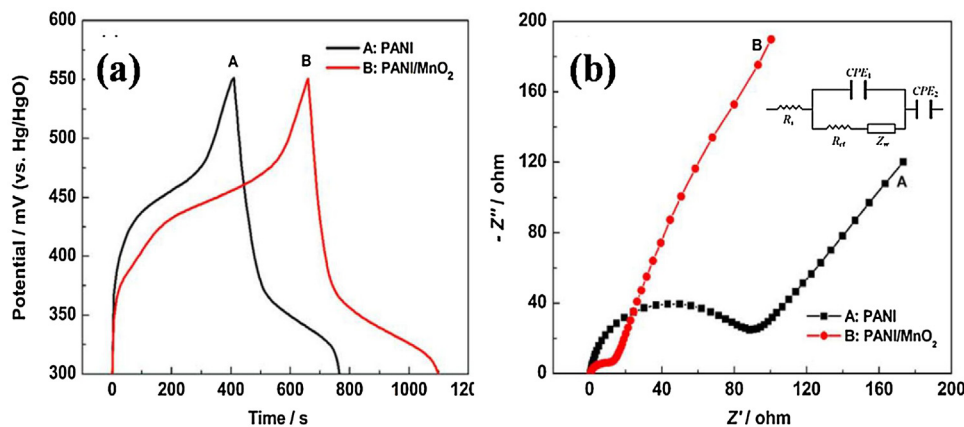
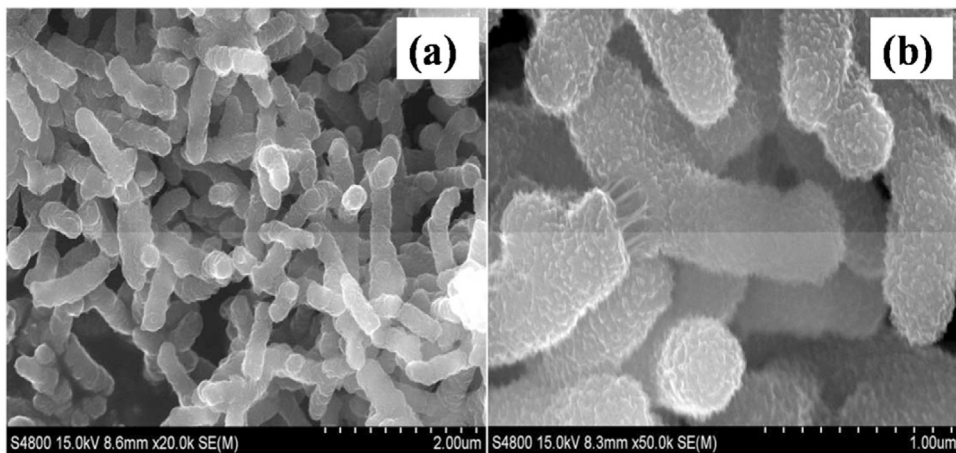


Fig. 4. (a) Galvanostatic CD curves of PANI and the PANI/MnO₂ composite at a current density of 0.5 A g⁻¹, and (b) Nyquist plots of the EIS for PANI and the PANI/MnO₂ composite, the inset is the equivalent circuit.

Reproduced from Ref. [54] with permission from John Wiley and Sons.

**Fig. 5.** SEM images of (a) PANI and (b) the PANI/MnO₂.

Reproduced from Ref. [54] with permission from John Wiley and Sons.

Table 2

Comparison of the supercapacitor properties of different metal oxide/polymer heterostructure.

Electrode materials	Electrolyte	Potential window (V)	Specific capacitance (F g ⁻¹)	Current density (A g ⁻¹)	Retention of specific capacitance	References
Ag/MnO ₂ /PANI	0.5 M LiClO ₄ + PC	-1 to 1	800	1	—	[49]
PANI/Fe ₃ O ₄	—	-0.2 to 1	213	1	~51% (5 A g ⁻¹)	[50]
Fe ₃ O ₄ @C@PANI	1 M KOH	-0.1 to 0.6	322.5	2.5	—	[51]
PANI/MnO ₂	0.5 N KOH	-1.2 to 1.2	210	50 mV s ⁻¹	—	[52]
Polyaniline/MnO ₂	1 M H ₂ SO ₄	-0.3 to 0.7	626	2	~76% (20 A g ⁻¹)	[53]
Polyaniline/MnO ₂	6 M KOH	0.3 to 0.55	810	0.5	~11% (4 A g ⁻¹)	[54]
Polyaniline/NiCo ₂ O ₄	0.5 M H ₂ SO ₄	0 to 0.7	439.4	5 mA cm ⁻²	~74% (20 mA cm ⁻²)	[55]

specific surface area. However, optimization of pore size and surface area is necessary for maximum utilization of ion adsorption. The specific capacitance of the carbonaceous materials was enhanced through the hybridization with different metal oxide and conducting polymers. On the other hand, graphene has a large specific surface area of ca. 2600 m² g⁻¹ which is substantially higher than those of the other carbonaceous materials. Two dimensional (2D) and atom-thick graphene is the most attractive EDLC electrode materials. However, the agglomeration of graphene sheets limits its application as supercapacitor materials. Hybridization of graphene or rGO with conductive polymers and metal oxide/hydroxide can prevent the agglomeration. On the other hand, this kind of hybridization enhanced the electrical conductivity of the metal oxides and polymers. CNTs also showed large specific surface area and excellent electrical conductivity. Many researchers reported on the hybridization of graphene, CNT, metal oxides and polymers leading to good quality electrode materials.

2.2.1. Hybridization of EDLC and metal oxide/hydroxide

The heterostructure of Iron oxide and carbonaceous materials were prepared through simple hydrothermal process [67–71]. Iron oxides (Fe₃O₄/Fe₂O₃) possess faradic charge storage mechanism through reversible redox reactions Fe²⁺ ↔ Fe³⁺ [60,63].

Yang et al. reported the hybridization of α-Fe₂O₃ mesocrystals/graphene, where iron substituted the oxygen functionalities on graphene by forming the Fe–O–C bonds [67]. The strong attachment of α-Fe₂O₃ on graphene sheet was confirmed from the long time ultrasonication. The specific capacitance was calculated as 306.9 F g⁻¹ at 3 A g⁻¹ current density and the coulombic efficiency was recorded as ~90%. Lee et al. showed the specific capacitance of α-Fe₂O₃ nano tube/graphene electrode was ~9 times higher than that of the bare α-Fe₂O₃ electrode [61]. α-Fe₂O₃ nano tubes contained hollow tubular structure and posses

a large surface area for reaction [69]. In addition, the incorporation of rGO afforded a proficient 2D conductive pathway for fast and reversible redox reaction. Enhanced current response in CV was noticed after the incorporation of rGO in α-Fe₂O₃ (Fig. 6a & b). The discharging time also increased significantly for α-Fe₂O₃ nano tube/graphene heterostructure as compared to the bare α-Fe₂O₃ nano tube electrode (Fig. 6c & d) [69].

Nickel based supercapacitor electrode caught significant attention due to the low cost and rich pseudocapacitive performance. Formation of heterostructure with graphene overcome the poor electrical conductivity of NiO and Ni(OH)₂ [81–94]. The electrochemical performances of NiO and Ni(OH)₂ were tested in 6 M KOH electrolyte [81–94]. The incorporation of graphene with NiO and Ni(OH)₂ provides facile charge transfer and ion adsorption during charging/discharging. Three-dimensional NiO/rGO heterostructure was developed through chemical precipitation method followed by annealing. The electrochemical performance of bare NiO, rGO and NiO/rGO heterostructure was compared in terms of CV, CD and EIS spectroscopy analysis [88]. The CV of graphene showed no redox peak while the CV of NiO showed prominent oxidation reduction peaks at ~0.35 and ~0.25 V [88]. The area of the CV curve of NiO/graphene electrode increases significantly due to the synergistic effect of faradic and EDLC charge storage mechanism. The discharging capacity of the NiO/graphene electrode was also much higher than that of the bare NiO and graphene. The enriched electrochemical performance of the heterostructure was further analyzed by EIS spectroscopy analysis and it was found that the solution and faradic charge transfer resistance of the NiO was improved through hybridization with graphene [88]. The accessibility of the electrolyte ions within the electrode materials was also improved by the incorporation of graphene in NiO [88]. Gao et al. studied the charge storage capacity of NiO/CNT composite with different content of NiO [89]. The

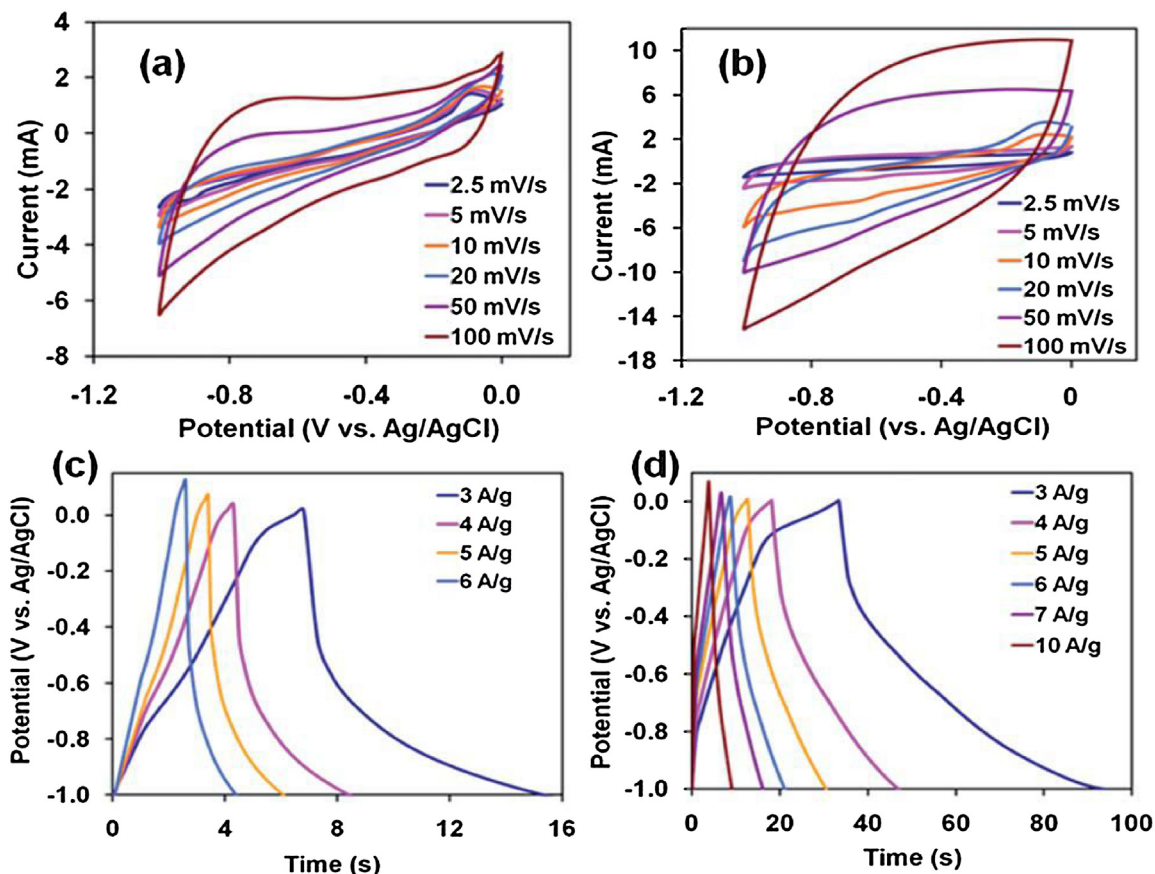


Fig. 6. CV curves of (a) α -Fe₂O₃ NTs, (b) α -Fe₂O₃ NTs-rGO at different scan rates and galvanostatic charge–discharge curves of (c) α -Fe₂O₃ NTs, (d) α -Fe₂O₃ NTs-rGO electrodes at different current densities in 1 M Na₂SO₄. Reproduced from Ref. [69] with permission from Royal Society of Chemistry

specific capacitance of NiO/CNT increased with decreasing content of NiO. The specific capacitance of NiO/CNT was calculated as 304.7 and 523.37 F g⁻¹ at 100 and 50 wt% of NiO, respectively [81]. However, the specific capacitance decreased to 382.84 F g⁻¹ (40 Wt %) with further decrease in NiO content. Heterostructure of Ni(OH)₂ and highly oxidized graphene exhibited very high specific capacitance of 1236.4 F g⁻¹ at 1.0 mV s⁻¹ scan rate.86 CD performance of highly oxidized graphene heterostructure was studied

with a varied range of current density of 0.1–10 A g⁻¹ and the Ni(OH)₂ and showed very high retention of 52.2%.

Superior electrochemical properties were achieved by the formation of heterostructure of MnO₂ and carbonaceous EDLC materials. MnO₂ exhibited rich pseudocapacitive properties [95–103]. In addition, low cost and environment compatibility of MnO₂ established it most popular electrode materials for energy storage applications. Many researchers modified the electrochemical

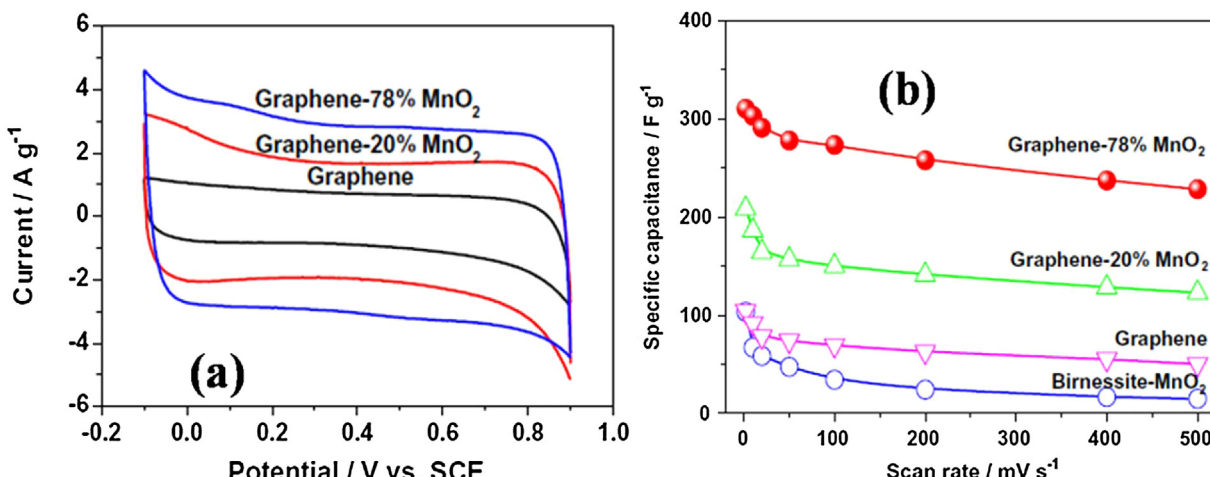


Fig. 7. (a) CV curves of graphene and graphene-MnO₂ composites at 10 mV s⁻¹ and (b) Specific capacitance (based on the composite) at different scan rates of 2, 10, 20, 50, 100, 200 and 500 mV s⁻¹ in 1 M Na₂SO₄ solution. Reproduced from Ref. [95] with permission from Elsevier.

properties of MnO_2 through hybridization with graphene or rGO. The electrochemical properties such as current response, specific capacitance and the retention of capacitance of the graphene/ MnO_2 heterostructure electrode depend on the wt% of graphene in the composite. Yan et al. compared the electrochemical performance of bare graphene, MnO_2 and graphene/ MnO_2 with different content of graphene through CV analysis. Current response of graphene/ MnO_2 heterostructure was much better than the bare graphene (Fig. 7a) [95]. The retention of specific capacitance of graphene/ MnO_2 composite was also high as compared to the bare graphene and MnO_2 (Fig. 7b) [95]. Highest electrochemical properties were achieved with ~78% loading of graphene. It was found that the structural properties of the carbonaceous materials like rGO and CNT changed in the composite materials due to the incorporation of the metal oxides and metal ions. In addition, the surface electronic properties of rGO destroyed due to the formation of heterostructure. However, the presence of metal oxides played the role of spacer materials in between the rGO sheets and prevented the agglomeration and at the same time increased the available electrochemically active surface area of rGO.

Li et al. prepared graphene/ MnO_2 composite papers for flexible supercapacitor electrode [96]. Graphene/ MnO_2 composite papers were advantageous due to its freestanding nature and binder free preparation method. Chen et al. prepared heterostructure of GO supported by needle like MnO_2 [100]. The basal planes of GO sheets are decorated with epoxy and hydroxyl groups. On the other hand, the edge of GO consisted of carbonyl and carboxyl groups. All these functional groups played the role of anchor sites by allowing in situ formation of nanostructures on the surfaces and edges of GO sheets. The crystalline structure of MnO_2 consisted with basic MnO_6 octahedron units, which produced different crystallographic morphology of MnO_2 during the hybridization with GO [100]. The growth mechanism of metal oxides was different in presence of carbonaceous materials. Graphene or rGO acted as a platform for the deposition of the metal oxide particles on the surface. As a result, nano sized particles of metal oxide was formed. On the other hand, the charge storage mechanism of the metal oxides is not only the surface properties. Rather the charge transfer of the metal oxides was related to the amount of active site present in the bulk materials. However, bare metal oxides possess low specific capacitance, as the total active site of the electrode materials was not exposed to the electrolyte ions. The rGO present in the heterostructure of electrode materials played synergistic effect by providing the EDLC as well as enlarging the exposed active sites of the metal oxides. As a result, the specific capacitance as well as rate

capability of the metal oxides increased significantly due to the presence of carbonaceous materials.

Layer-by-layer assembly of MnO_2 and rGO were carried out through successive ionic layer adsorption and reaction (SILAR) method [104]. Additive-free electrode was prepared on a stainless steel current collector. The electrochemical performance of the MnO_2 /rGO electrode produced by SILAR method was compared with another electrode developed by hydrothermal method. It was noticed that the special orientation (layer-by-layer assembly) of the MnO_2 and rGO generates superior supercapacitor performance as compared to the hydrothermally prepared electrode [104]. Fig. 8a shows the FE-SEM image of MnO_2 /rGO (SILAR) electrode. MnO_2 nano rods were uniformly distributed over the exfoliated rGO sheets. Fig. 8b shows the specific capacitance vs. current density plot of pure MnO_2 , MnO_2 /rGO (hydrothermally produced) and MnO_2 /rGO (SILAR), respectively. It was found that the specific capacitance of MnO_2 /rGO (hydrothermally produced) was almost twice than the pure MnO_2 . Specific capacitance was improved further (almost twice) when electrode was prepared by SILAR method [104]. Generally, the metal oxides are large band gap semiconductor with low electrical conductivity. Conversely, graphene, rGO and CNT are highly electrically conducting. As a result, the electrical conductivity of the metal oxides/EDLC composites was found to be much higher than the bare metal oxides. The enhancement in the electrical conductivity decreased the solution or series resistance of the heterostructure electrode. Low series resistance is advantageous for supercapacitor applications due to the small internal loss and high rate capability.

Apart from manganese, nickel and iron based metal oxides, many researchers prepared the heterostructure of carbonaceous materials with other metal oxides like (RuO_2 , Co_3O_4 and V_2O_5 etc) [105–114]. Variable oxidation states and superior faradic activity of these metal oxides were further modified with fast charge/discharge, enlarged surface area and high retention by hybridization with carbonaceous materials like rGO, graphene and CNT [105–114]. The supercapacitor properties of different EDLC/metal oxide based electrode are compared in Table 3. The supercapacitor properties were evaluated in KOH or Na_2SO_4 electrolyte. Ni and Fe based materials were studied in KOH electrolyte. On the other hand, the electrochemical properties of MnO_2 based materials were evaluated in Na_2SO_4 electrolyte. The specific capacitance of Ni based materials was higher in KOH electrolyte. On the other hand, MnO_2 showed large potential window in Na_2SO_4 electrolyte. It was found that the higher potential window was achieved by using Na_2SO_4 electrolyte.

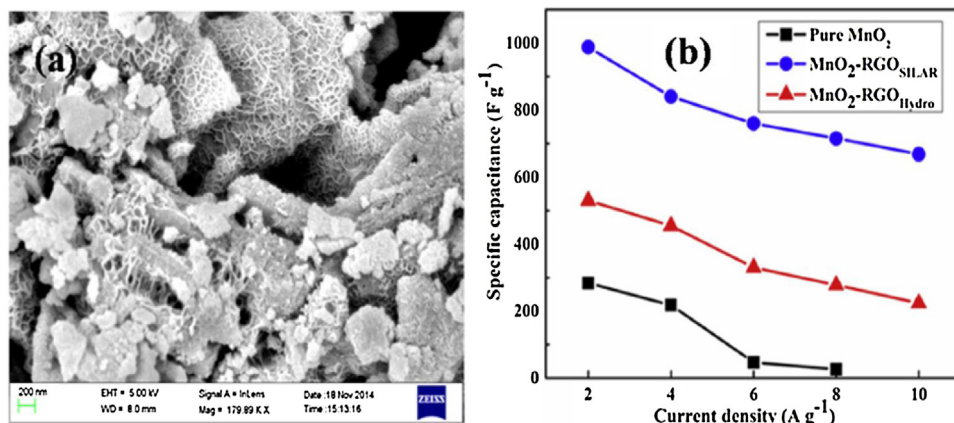


Fig. 8. (a) FE-SEM image of MnO_2 /rGO (SILAR) and (b) Gravimetric specific capacitance vs. current density of pure MnO_2 , MnO_2 /rGO (SILAR) and MnO_2 /rGO (Hydrothermal). Reproduced from Ref. [104] with permission from Elsevier.

Table 3

Supercapacitor properties of different types of metal oxide heterostructure electrode materials.

Electrode materials	Electrolyte	Potential window (V)	Specific capacitance (F g^{-1})	Current density (A g^{-1})	Retention of specific capacitance	References
Fe ₂ O ₃ /Graphene aerogel	PVA/KOH	−1.1 to −0.1	440	0.45	~89% (1.5 A g^{-1})	[68]
α-Fe ₂ O ₃ /rGO	0.1 M K ₂ SO ₄	−1 to 0	215	2.5 mV s^{-1}	~52% (20 mV s^{-1})	[69]
Fe ₂ O ₃ /Graphene aerogel	0.5 M Na ₂ SO ₄	−0.8 to 0.8	81.3	1	~77% (10 A g^{-1})	[70]
Fe ₃ O ₄ /rGO	0.5 M Na ₂ SO ₄	0 to 0.8	154	1	—	[71]
NiO/rGO	6 M KOH	−0.4 to 0.5	461	0.21	~67% (4.17 A g^{-1})	[81]
NiO/rGO	6 M KOH	0 to 0.5	428	0.38	—	[83]
Graphene/NiO	6 M KOH	−0.1 to 0.4	525	0.2	~62% (6 A g^{-1})	[84]
Graphene/NiO	2 M KOH	0 to 0.5	346	1.5	—	[88]
NiO/CNTs	6 M KOH	−0.1 to 0.4	523.37	5 mA cm^{-2}	~43% (20 mA cm^{-2})	[89]
NiO/CNTs	1 M KOH	0 to 0.65	1329	84	—	[91]
Ni(OH) ₂ /Graphene	6 M KOH	−0.1 to 0.45	1735	1 mV s^{-1}	~30% (50 mV s^{-1})	[92]
Ni(OH) ₂ /Graphene	1 M KOH	0 to 0.55	1335	2.8	~71% (45.7 A g^{-1})	[93]
MnO ₂ /Graphene	1 M Na ₂ SO ₄	−0.1 to 0.9	310	2 mV s^{-1}	~73% (500 mV s^{-1})	[95]
MnO ₂ /Graphene		0 to 1	230	50 mV s^{-1}	~82% (500 mV s^{-1})	[97]
MnO ₂ /Graphene	1 M Na ₂ SO ₄	0 to 0.8	422.5	1	~54% (10 A g^{-1})	[98]
MnO ₂ /Graphene	1 M Na ₂ SO ₄	−0.1 to 0.9	310	2 mV s^{-1}	~92% (500 mV s^{-1})	[99]
MnO ₂ /Graphene	1 M Na ₂ SO ₄	0 to 1	216	0.15	~51% (1 A g^{-1})	[100]
MnO ₂ /Graphene	1 M Na ₂ SO ₄	−0.1 to 0.9	350	0.2	~46% (10 A g^{-1})	[102]
MnO ₂ /Graphene	PVA/H ₃ PO ₄	−0.7 to 0.7	254	0.5	~83% (10 A g^{-1})	[103]
Co ₃ O ₄ /rGO	2 M KOH	0 to 0.8	472	2 mV s^{-1}	~82.6% (100 mV s^{-1})	[107]
Co ₃ O ₄ /rGO	6 M KOH	0 to 0.8	163.8	1	~87% (10 A g^{-1})	[108]
Co ₃ O ₄ /Graphene	0.1 M NaOH	0 to 0.7	768	10	~59% (30 A g^{-1})	[109]
Co ₃ O ₄ /Graphene	6 M KOH	−0.1 to 0.5	341	10 mV s^{-1}	~30% (200 mV s^{-1})	[110]
V ₂ O ₅ /graphene/MWCNT	1 M Na ₂ SO ₄	−1 to 1	504	0.5	~40% (10 A g^{-1})	[119]

2.2.2. Hybridization of EDLC and conducting polymers

Accurate control over the nanoscale dimension and morphology of conducting polymers is necessary in recovering the performance of pseudocapacitors. Due to their unique electrochemical properties and small dimensions, conducting polymer nanostructures have finds wide range of applications [115–118]. In

addition, conducting polymers possess reversible electrochemical doping-dedoping for improved electrochemical performance. In order to synthesize new types of hybrid materials various conducting polymer precursors was used. The morphology and structure of the heterostructure materials can be controlled with varying the polymer precursors. Various researchers reported the

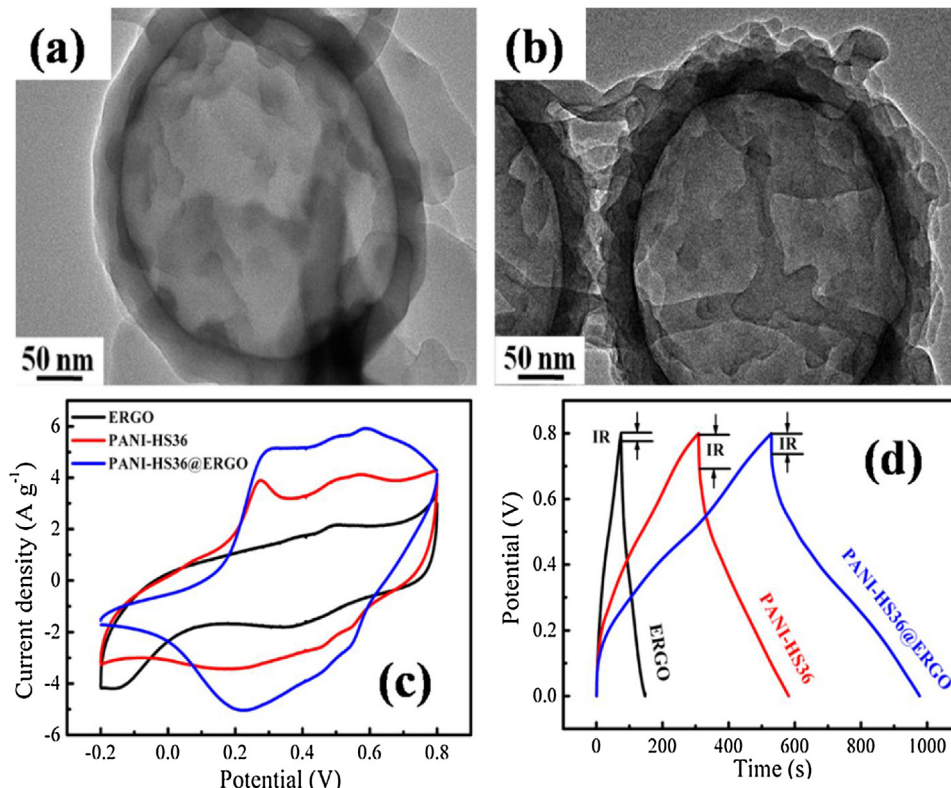


Fig. 9. TEM images of (a) PANI-HS80, (b) PANI-HS36@GO hybrids, (c) CV curves of ERGO, PANI-HS36, and PANI-HS36@ERGO hybrids at a scan rate of 10 mV s^{-1} in 1 M H₂SO₄ solution and (d) Galvanostatic charge-discharge curves of ERGO, PANIHS36, and PANI-HS36@ERGO hybrids within a potential window of 0–0.80 V at a current density of 1 A g^{-1} .

Reproduced from Ref. [120] with permission from American Chemical Society.

formation of the heterostructure electrode of GO/polypyrrole (PPy) and GO/polyaniline (PANI) [115–118]. The hybridization leads to high surface area and electroactive regions along with short diffusion path [119–125]. Elevated surface area provides rich EDLC characteristic. Furthermore, the availability of the redox active sites also increases with increasing specific surface area.

Hybridization of PANI with rGO/graphene provides facile electrical pathway, which improved the faradic charge storage mechanism [118–125]. Fan et al. reported the electrochemical synthesis of graphene-wrapped PANI hollow spheres for energy storage application [120]. Fig. 9(a & b) shows the TEM images of PANI hollow spheres and graphene-wrapped PANI hollow spheres, respectively. The wrapping of rGO sheets on the PANI- put forward a highly conductive path, thus providing superior electrochemical performance of the electrode. The area of the CV curves of rGO-wrapped PANI hollow spheres increased as compared to the bare rGO and PANI hollow spheres (Fig. 9c). The discharging time increased due to the hybridization of two different EDLC and pseudocapacitance materials (Fig. 9d) [110]. The specific capacitance of PANI/rGO heterostructure was calculated as 614 F g^{-1} at a current density of 1 A g^{-1} [120]. Yan et al. prepared the heterostructure of PANI/graphene nano sheets for supercapacitor applications [122]. PANI/graphene nano sheets showed high specific capacitance of 1046 F g^{-1} at 1 mV s^{-1} scan rate. The stability of the electrode was increased significantly with the addition of 1 wt% of CNT within the graphene nano sheets [122]. Wang and co-workers deposited PANI nano wires on the polystyrene microsphere/rGO through dilute polymerization and

then removed the polystyrene microsphere to form freestanding PANI/rGO electrode [125]. 3D PANI/rGO heterostructure provided large interfacial area, shorten ion diffusion path and facile electrical pathways, thus providing full use of electroactive sites. Furthermore, the high electrical conductivity of graphene as well as strong π electron interaction between PANI and rGO reduced the charge-transfer resistances of the heterostructure film. As a result the specific capacitance (740 F g^{-1}) and cycling stability of the 3D PANI/rGO electrode was improved significantly as compared to bare PANI [125].

PPy is widely used as the pseudocapacitive materials in supercapacitor applications. Superior electrical conductivity, mechanical flexibility and high redox activity of PPy established it as the appropriate materials for flexible supercapacitor electrode [126–133]. However, the practical application of PPy is limited due to the poor stability and retention. Hybridization of PPy with carbonaceous materials enhanced the electrochemical property by providing a backbone of EDLC [126–133]. Li and co-workers prepared paper like film where PPy fibres were evenly distributed within the graphene sheets [126]. Fig. 10(a &b) showed the morphology of rGO/PPy heterostructure. The distribution of PPy fibres created interspaces in between the rGO layers and prevented the restacking in comparison to pure rGO. PPy fibres were covered by the rGO sheets providing enlarged surface areas with huge amount of concaves and convexities. The CV of the PPy, rGO and rGO/PPy heterostructure was compared at 50 mV s^{-1} scan rate (Fig. 10c). Significant increase in the current response of rGO/PPy heterostructure as compared to the bare rGO and PPy suggested

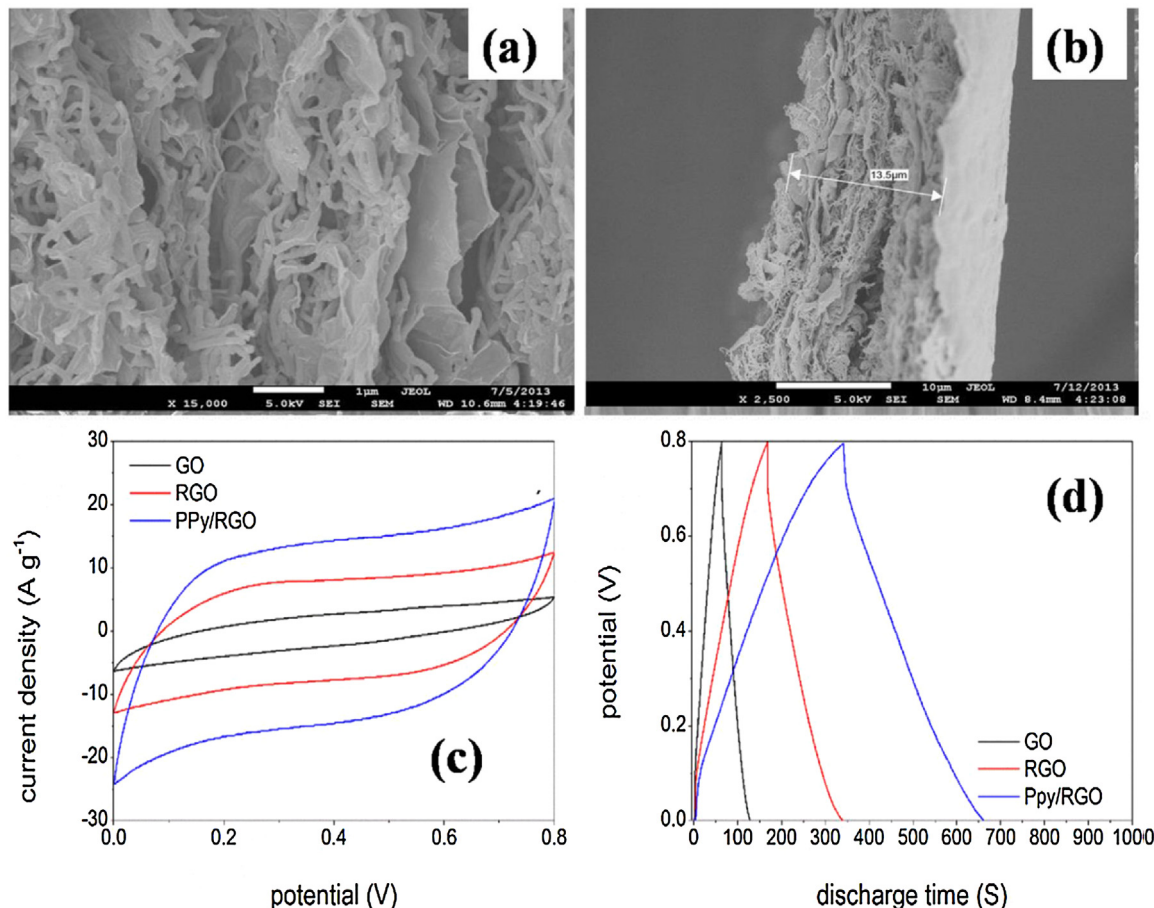


Fig. 10. FE-SEM images showed (a) localized cross section of the area, which defined by the pane (b) thickness of PPy fibre/RGO film, (c) Cyclic voltammogram curves of capacitors using $\text{H}_3\text{PO}_4/\text{PVA}$ gel as electrolyte with different flexible electrodes at the scan rate of 50 mV s^{-1} , (b) Galvanic discharge curves at 1 A g^{-1} . Reproduced from Ref. [126] with permission from Elsevier.

improved electrochemical activity due to the hybridization of two different active materials. The discharging time of the rGO/PPy heterostructure increased in comparison to the bare rGO and PPy (Fig. 10d) [126]. The specific capacitance of rGO/PPy heterostructure was measured as 345 F g^{-1} at 1 A g^{-1} current density.

Chen et al. reported the tuning of the surface property of graphene through hybridization with PPy [131]. The distribution of PPy on rGO provided synergistic effect by preventing restacking and creating short diffusion pathway for the electrolyte ions [131]. Furthermore, the PPy/rGO based supercapacitor showed excellent rate capability, long life stability and high areal capacitance of 2.61 mF cm^{-2} . In addition, PPy/rGO electrodes exhibited excellent flexibility and high mechanical stability. Davies and co-workers reported a simple pulsed electro-polymerization method to design flexible and uniform graphene/PPy films for supercapacitor applications [133]. The graphene/PPy electrode exhibited additional pseudocapacitive contribution along with the inherent flexibility of graphene. Formation of favourable nucleation of new polymer chains on the graphene surface provided high specific capacitance of 237 F g^{-1} at a scan rate of 10 mV s^{-1} .

2.3. Doping of the supercapacitor electrode materials

The electrochemical performances of metal oxides, polymers and carbonaceous materials can be improved significantly through doping. The presence of heteroatom generates free electron, electro chemically active sites and enhanced the surface area of the electrode materials. Generally the specific capacitance of the EDLC materials increases as the result of doping. On the other hand, the rate capability and stability of the pseudocapacitance materials can be improved by doping. Both the p and n type doping of the supercapacitor materials was extensively studied for supercapacitor applications. The electrochemical properties of the doped electrode materials are summarized in Table 4.

2.3.1. Doping of the EDLC electrode materials

The electrochemical properties of the carbonaceous electrode materials were significantly improved by doping with heteroatom such as oxygen, nitrogen, and boron [134–142]. These kinds of heteroatoms acted as donor or acceptor by generating additional electrons and holes while incorporated with carbon. Among the heteroatoms, nitrogen is the most superior dopant with five valence electrons due to which it plays the role of electron donor in

the carbon lattice. N doping shifted the Fermi level carbon electrodes to the valence band [135]. Furthermore, the N doping within the carbon moiety enhanced the wettability of the electrolyte/electrodes interface. Chen et al. prepared N doped spherical carbon through a template carbonization method, where polyacrylamide (PAM) serves as the source of C and N, and calcium acetate acts as hard template [136]. It was observed that the mass ratio of polyacrylamide and calcium acetate have crucial impacts upon both the pore structures as well as capacitive performance [136]. N doped carbon spheres had low-graphitization degree and showed a BET surface area of $648 \text{ m}^2 \text{ g}^{-1}$ along with the pore volume of $0.59 \text{ cm}^3 \text{ g}^{-1}$. The specific capacitance was calculated as 194.7 F g^{-1} at a current density of 0.5 A g^{-1} [136]. The retention of specific capacitance was also very high (97.8%) after 5000 CD cycles. Peng and co-workers developed N doped carbon network through integrated oxidation polymerization and catalytic carbonization technique [140]. The as-synthesized N doped 3 D carbon exhibited porous framework architecture along with large specific surface area. In addition, high N content carbon network provided fast electron transfer throughout the electrode and showed high specific capacitance of 304 F g^{-1} [137]. Furthermore, the N doped porous carbon showed excellent rate capability and high cycling stability (only 3% capacitance loss) performance up to 5000 CD cycles [137]. The atomic size of C and N are quite similar. As a result N can easily replace the C atoms. The creation of free electros due to the N doping can take part in the electrochemical charge transfer. Thus the stability and the rate capability of the carbon electrode increased after doping.

On the other hand, graphene is sp^2 -bonded carbon atoms due to the hybridization of s, p_x and p_y atomic orbitals, which formed three sturdy σ bonds with the adjacent atoms [130]. However, there is another p_z orbital remained on each carbon which overlaps with those from neighbouring atoms and established a filled and empty band called π and π^* orbitals, respectively. Due to these valance (filled) and conduction (empty) band of orbitals, graphene is considered as zero band gap semiconductor or metal with vanishing Fermi surface. In this respect, the application of graphene is highly restricted in the field of electrochemistry or energy storage, due to the lack of intrinsic band gap. Introduction of a small band gap is promising way to advance the aforementioned applications [140–147]. In addition, new electronic properties were achieved by forming various morphologies of graphene, including zero-dimensional graphene and graphene quantum dots.

Table 4

Comparison of the supercapacitor properties of different electrode materials before and after doping.

Electrode materials	Doping elements	Specific capacitance before doping (F g^{-1})	Specific capacitance after doping (F g^{-1})	Corresponding current density (A g^{-1})	References
Porous Carbon	Nitrogen	–	194.5	0.5	[136]
Porous Carbon	Nitrogen	–	304	0.5	[137]
Graphene	Nitrogen	107	128	1	[150]
Graphene	Nitrogen	98	210	1	[151]
Graphene	Nitrogen	90.93	131.17	10 mV s^{-1}	[152]
Graphene	Nitrogen	133.7	246.4	1	[153]
Graphene paper	Nitrogen	29	280	5 mV s^{-1}	[154]
Graphene	Boron	–	200	0.1	[157]
CNT	Nitrogen	42	146	10 mV s^{-1}	[160]
CNT	Nitrogen	69	215	0.2	[161]
Carbon/CNT	Phosphorus	100	220	1	[162]
AC	K ⁺	32	431	10 mV s^{-1}	[165]
rGO/h-BN	Fluorine	942	1250	10 mV s^{-1}	[164]
MnO ₂	Nickel	150	194	0.005	[166]
NiO	Cobalt	–	1982	5 mV s^{-1}	[167]
NiO	Lanthanum	127	253	3 mV s^{-1}	[169]
NiO	Cu ²⁺	318	372	10 mV s^{-1}	[170]
Ni(OH) ₂	Cobalt	–	1421	6	[171]
CuS	Iron	328.26	516.39	5 mV s^{-1}	[172]

Generally, two types of chemical doping were extensively investigated. In surface transfer doping the heteroatoms adsorb on the surface without forming sp^3 defects within graphene lattice [145]. On the other hand, substitution doping of foreign atoms formed sp^3 defect regions by upsetting the sp^2 network through covalent bonding.

Luo et al. explored the electrical conductivity, diffusion behaviours and charge storage mechanism of graphene sheets with different hole defects or nitrogen doping [146]. It was noticed that graphene sheets contained pyridinic-like holes, which has hexagonal structure, was doped more easily with nitrogen and maintained excellent mechanical properties [146]. The mechanical stability of the electrode materials is beneficial for long life stability. Furthermore, N doping donates electrons, which in turn leads to accumulation of charges and produces higher pseudocapacitance. N is more electronegative (3.04) than that of C (2.55) and creates polarization within the carbon network. This kind of polarization generated superior electrochemical properties of graphene [145]. N in the graphene moiety showed three different bonding configurations including pyridinic, pyrrolic, and graphitic-N [148,149]. These three bonding system have different binding energy. There are several examples of the improvement of charge storage capacity of graphene through N doping [17,150–154]. Jeong et al. prepared N doped graphene through a simple plasma process and design supercapacitor device, which showed at least 4 times improved electrochemical property as compared to the pristine graphene sample [17]. N doped graphene exhibited excellent cycle stability ($>2,00,000$), elevated power capability, and high compatibility with flexible substrates. The morphology of the electrode material was studied with SEM images which showed homogeneous and porous distribution of graphene sheets. The superior electrochemical properties of the N doped graphene were raised

due to even distribution of the N atoms between edges and basal planes [17]. The difference in electronegativity of N and C changed the polarity of the C—N in the doped graphene. As a result, the presence of N in the graphene moiety provided additional charge storage capacity due to the chemisorption of the electrolyte ions. The chemisorption of the electrolyte ions increased the current response of the electrode materials. In addition, different electronic structure of N and C created free charge carriers when forming hetero structure. As a result, N doped graphene showed facile charge transfer in comparison to the un-doped graphene.

Wang and co-workers prepared N-doped few layer graphene with crumpled morphology for supercapacitors application [150]. Fig. 11a shows the SEM image of crumpled few layer graphene. The 2D crumpled graphene nanosheets (CNG) possess large ion-available surface area, superior electron/ion diffusion property and high packing density. Fig. 11b showed the CV of pure graphene sheet (GS), rGO and CNG at 10 mV s⁻¹ scan rate [150]. N doping provided high current response as compared to the pure GS. The specific capacitance of CNG was very high as compared to the bare GO and GS (Fig. 11c). In addition, the series resistance and the charge transfer resistance of the graphene improved after N doping (Fig. 11d) [150]. Outstanding volumetric capacitance of (98 F cm⁻³) of N doped graphene was ascribed to the synergistic effect efficient EDLC as well as superior ion-accessible surface. Furthermore, several researchers also reported the high retention and long life stability as the result of N doping in graphene [152–154]. Li et al. developed high performance (280 F g⁻¹) supercapacitor with N-doped graphene, which showed excellent (99.4%) stability after 40,000 cycles [154]. The higher specific capacitance of the N doped carbonaceous materials can be attributed to the improved electrical conductivity as well as low series and charge transfer resistance of the electrode materials. Doping is also helpful for the

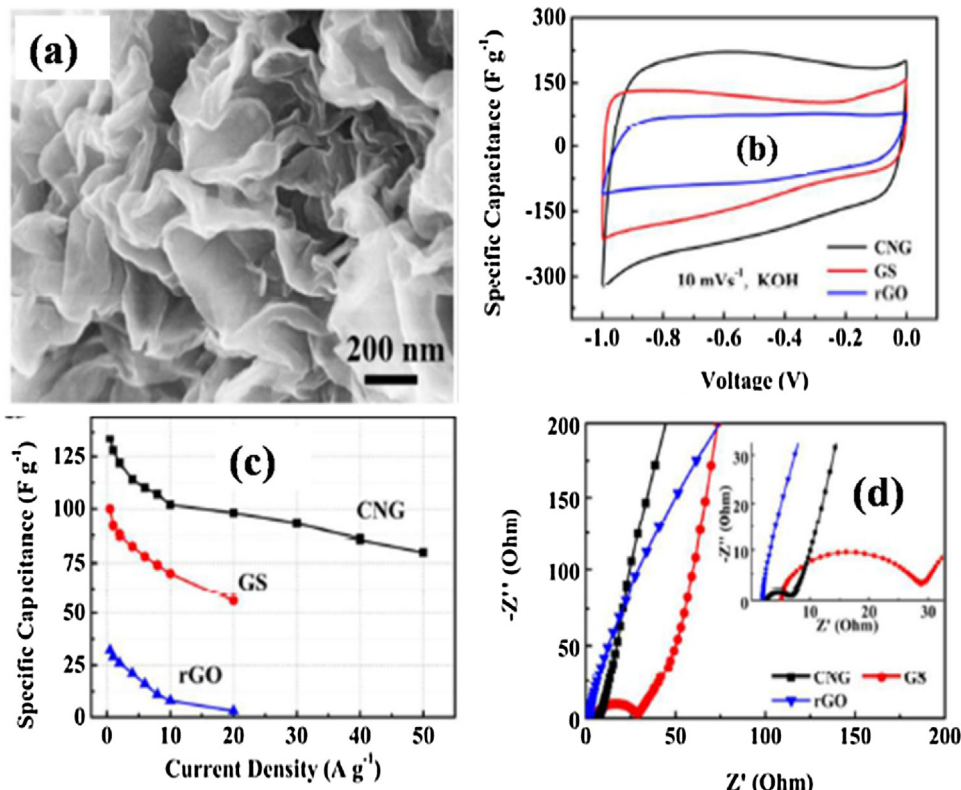


Fig. 11. (a) SEM image of CNG, (b) CV plots of different electrodes in a three-electrode system with 6 M KOH electrolyte, (c) Specific capacitances of different graphene-based supercapacitors at various current densities in EMImBF₄ electrolyte, and (d) Nyquist plots of different electrode. Reproduced from Ref. [150] with permission from American Chemical Society.

facile diffusion of the electrolyte ions. High diffusion rate reduced the Warburg charge transfer resistance due to the decreased in the diffusion time constant. Nie et al. reported the superior supercapacitor performance of carbon materials with high content of N and O functionalities [141]. In addition, the incorporation of novel redox additives in to the electrolyte was an effective way for the enhancement of specific capacitance of carbon based materials [141,142]. The superposition of potential window due to the presence of redox additives was the reason of increased specific capacitance of carbon based electrodes.

Doping of graphene with B is another way to improve the electrochemical properties of graphene. Although, In-plane B doping is advantageous because B atoms are sp^2 hybridized within the carbon lattice, which allows the planar structure of graphene [146,155,156]. However, B-doping at the vacant sites created distortion due to the saturation of the dangling carbon atoms in tetrahedral-like BC₄ unit [146,155,156]. Han et al. showed excellent electrical property and enlarged surface area of the B doped rGO [157]. The specific surface area of the B doped rGO was calculated as $466\text{ m}^2\text{ g}^{-1}$. In addition, the high specific capacitance of 200 F g^{-1} and long stability was also achieved as a result of B doping [157]. Peng and co-workers developed flexible boron doped graphene through laser induction process and design a micro supercapacitor for energy storage application [158]. It was observed that areal capacitance was almost three times increased

(16.5 mF cm^{-2}) after boron doping. In addition, the flexibility and cyclability of the micro supercapacitor did not hampered due to the boron doping. Doping created effective pathway for electron or ion transfer due to which the electrical conductivity can be enhanced. The electronegativity of B and C also different thus formed a quasi-polar bond. Thus chemisorption of the electrolyte ions on the carbon surface increased the overall specific capacitance of the B-doped graphene.

The doping of CNT was extensively studied for supercapacitor applications [159–163]. N doping introduced pseudocapacitance property within CNT [159]. The specific capacitance was varied with different content of hetero atoms. Maximum specific capacitance (190.8 F g^{-1}) was achieved at 9.1 wt% of nitrogen doping [159]. Very high capacitance retention (94.5%) was noticed after 10,000 CD cycles. Patino and co-workers prepared phosphorus (P)-doped carbon-CNT hierarchical monoliths for supercapacitor application [162]. P-doped CNT hetero structure exhibited high specific capacitance of $\sim 220\text{ F g}^{-1}$ which was more than two times larger than that of the un-doped CNT. The capacitance retention was very high even when the discharging current density increased by 40 times.

Doping of alkali or alkaline-earth metals like potassium (K) in to the carbon structure advantageous for supercapacitor applications [165]. The incorporation of K generates extra charge which fill the π^* states of carbon. As a result the electrical conductivity increased

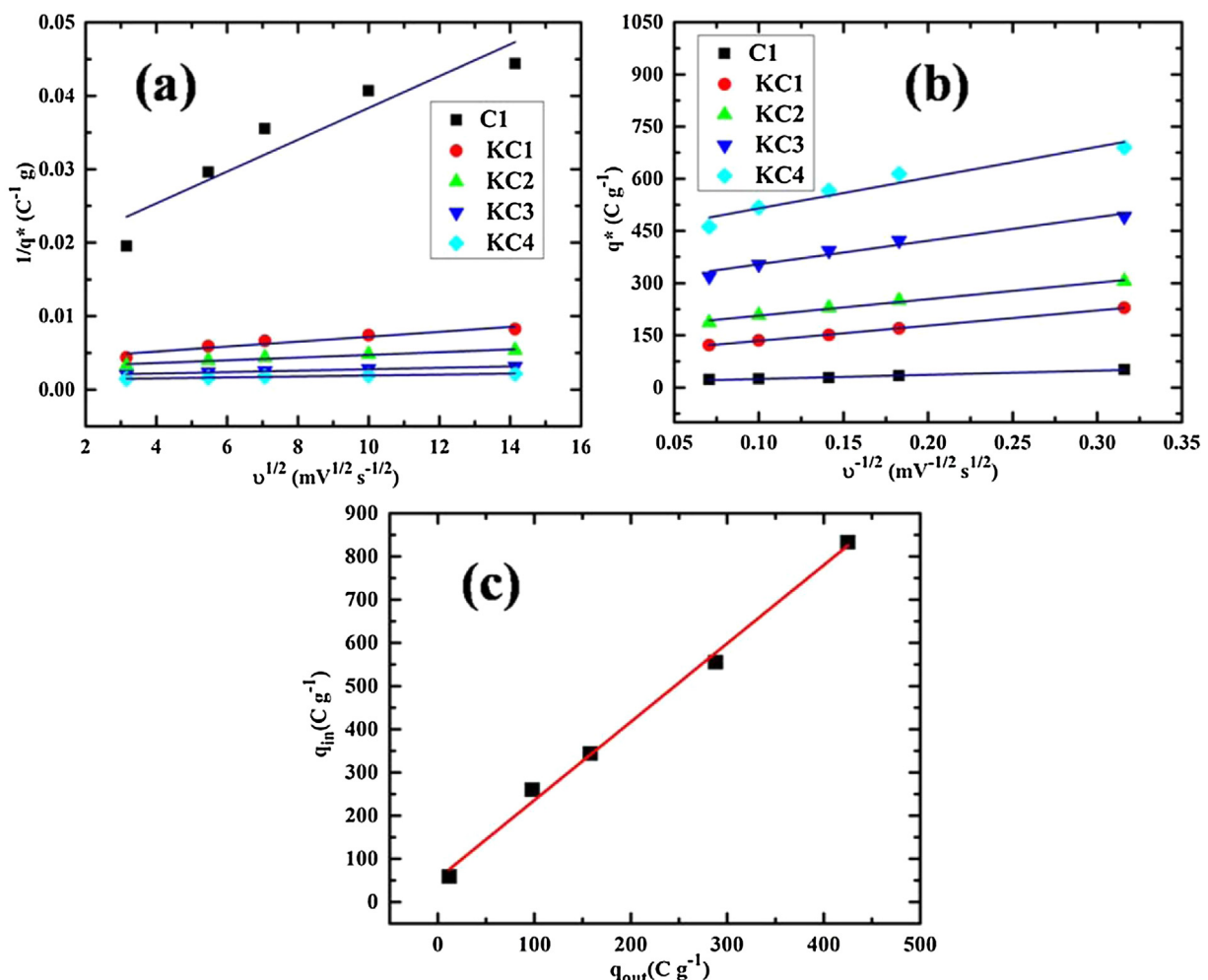


Fig. 12. Variation of the voltammetric charge (q^*) with respect to the sweep rates v : (a) extrapolation of q^* to $v = 0$ from the $1/q^*$ versus the $v^{1/2}$ plot, (b) extrapolation of q^* to $v = \infty$ from the q^* versus $1/v^{1/2}$ plot, and (c) Linear fitted q_{in} versus q_{out} plot of C1, KC1, KC2, KC3, and KC4. Reproduced from Ref. [165] with permission from American Chemical Society.

significantly [165]. Saha et al. showed the increase in the density of states due to the K doping in the activated nano-graphitic structure derived from Cotton (*Gossypium arboreum*). Surface area ($162.7 \text{ m}^2 \text{ g}^{-1}$) of the K-doped activated carbon increased significantly as compared to the un-doped sample ($10.2 \text{ m}^2 \text{ g}^{-1}$) [165]. In addition, the effective active sites (easily available outer active sites) of the electrode materials enhanced as compared to the inner active sites (difficult to access by the electrolyte ions) in consequence to K incorporation.

Fig. 12a & b shows the variation of the voltammetric charge (q^*) with respect to the sweep rates v . q^* is varied directly with active surface area and inversely with scan rate. q^* has two separate regions, 1st outer surface voltammetric charge (q^*_{out}) and 2nd the inner surface voltammetric charge (q^*_{in}). It was noticed that the value of q^*_{in} was always higher than the q^*_{out} for all the doped and un-doped samples. However, the percentage of accessible active surface increases with increasing doping concentration. **Fig. 12c** represents the variation of the charge densities with q^*_{out} and q^*_{in} . The q^*_{out} to q^*_{in} ratio of dope-activated carbon (~52%) was significantly higher than that of un-doped sample (~21%). The K doped activated carbon exhibited a high specific capacitance of 431 F g^{-1} at 10 mV s^{-1} scan rate [165].

2.3.2. Doping of the redox materials

It is well known that the electrical conductivity of electrode materials is an important factor for high performance supercapacitor applications. However, metal oxides and conducting polymers suffers from poor electrical conductivity, which limits the ion and electron transfer. Especially, these drawbacks become more crucial during high CD rate where most of the volume or active sites remain useless and specific capacitance of the electrode decreases. Thus, it is imperative to recover the electrical conductivity of metal oxide and polymers in order to achieve

high supercapacitive performance. Doing with heteroatom is one effective approach in this regard.

2.3.2.1. Doping of the metal oxide/hydroxide electrode materials. Zhian et al. studied the effect of Ni-doping on the electrochemical properties of MnO_2 [166]. Ni-doped MnO_2 was synthesized by using a solid-state reaction route where the reduction of KMnO_4 was carried out with manganese acetate and nickel acetate at low temperature. The morphology of the heterostructure was varied with different dopant content. It was noticed that the dimension of the synthesized materials were in nano meter range and the size were continually decreasing with increasing Ni content. The electrochemical properties enhanced with increasing Ni content. Maximum specific capacitance (194.5 F g^{-1}) was recorded at 20% molar fraction of Ni.

Heteroatom doping is also useful to enhance the electrochemical properties of the NiO [167–173]. Han et al. demonstrated the effect of La^{3+} -doping on the particle size, specific surface area and electrochemical properties of NiO [169]. The surface area of La^{3+} -doped NiO was calculated as $277.5 \text{ m}^2 \text{ g}^{-1}$ along with a large pore volume of $0.79 \text{ cm}^3 \text{ g}^{-1}$ [169]. The doping was confirmed from the microstructure observation. SEM and TEM images of La doped NiO is shown on **Fig. 13(a–c)**. **Fig. 13d** shows the corresponding FFT pattern. SEM image showed the uniform distribution of porous sphere of La^{3+} doped NiO . The average size was estimated as ~1–2 μm . TEM image showed the NiO spheres were little agglomerated and assembled in such a way that lots of porous channels were formed. The lattice spacing was calculated from the homogeneous and parallel lattice fringes of HR-TEM image [169]. The spacing was slightly larger than that of the (111) plane of pristine NiO suggesting the increasing interlayer distance due to doping [169]. The specific capacitance of La^{3+} doped NiO also increased by two times as compared to the pure NiO .

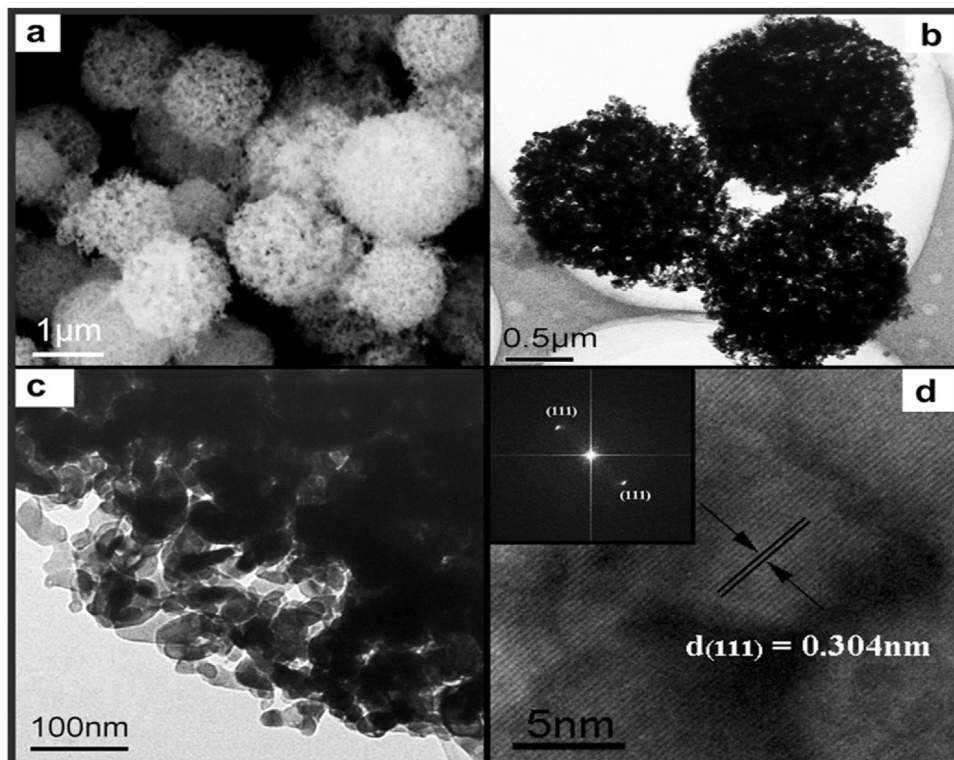


Fig. 13. (a) SEM, (b and c) TEM and (d) HR-TEM Images of 1.50 mol% La doped NiO . The insert is corresponding FFT pattern. Reproduced from Ref. [169] with permission from Elsevier Ltd.

Sathishkumar and co-workers showed the average size and shape of the NiO particles depended on the Cu²⁺ doping [170]. Doping concentration changed the NiO particles to nano rods. It was found that better supercapacitor properties were achieved with lower concentration of doping as compared to the higher concentration of Cu²⁺ [170]. Purushothaman et al. reported high specific capacitance (1982 F g⁻¹ at 5 mV s⁻¹ scan arte) of cobalt-doped NiO films with 5 wt% of doping concentration [167]. It was observed that doping generated a porous network as well as well-organized amorphous grain structure which effectively increased the specific capacitance by increasing the redox activity of the NiO film. Liang and co-workers improved the morphology and electrochemical properties of Ni(OH)₂ nano sheet by Co doping [169]. An environment friendly laser-induced method was used to dope Ni(OH)₂ nano sheet with Co from the precursor contained Co colloid and sodium thiosulfate [171]. The shape and surface area of the Co doped Ni(OH)₂ nano sheet was tuned by varying the concentration of sodium thiosulfate in the precursor. In addition, the Co-doped Ni(OH)₂ was renewed to Co-doped NiO through thermal decomposition. Co-doped Ni(OH)₂ exhibited high specific capacitance of 1421 F g⁻¹ at a 6 A g⁻¹ current density. The rate capability of the Co-doped Ni(OH)₂ was highly improved as compared to the pristine Ni(OH)₂. It was expected that partial substitution of Co²⁺ for Ni²⁺ in the metal hydroxide and oxide after doping, generates excessive free holes in the valence band. As a result, valance band conductivity was enhanced in Ni(OH)₂. On the other hand, the mesoporous network of the doped Ni(OH)₂ also expanded the electrode-electrolyte contact area and reduced the ion diffusion path for redox reaction. Synergistic effect from high conductivity and enlarged effective surface area were responsible for the superior electrochemical properties of the Ni(OH)₂ doped.

2.3.2.2. Doping of the conducting polymers. Ion can be inserted within the matrix of conducting polymers. This kind of doping induces high electrical conductivity by delocalizing the electrons

on the polymer chains [174,175]. Generally, the p-doping (positively-charged) and n-doping (negatively-charged) of the polymers were generated by oxidation and reduction process, respectively. The n-doping potential of the common conducting polymers such as PANI and PPy are much lower than the electrolyte reduction potential [3]. As a result PANI and PPy can only be p-doped for supercapacitor applications.

PANI can be doped with heteroatom like different metal, which leads to higher electrical conductivity and superior electrochemical properties [176–181]. Phadnis et al. reported that high specific capacitance of 333.16 F g⁻¹ was achieved by Cd-doped PANI as compared to the pure PANI electrode (223.3 F g⁻¹) at the scan rate of 1.5 mV s⁻¹ [178]. The electrical conductivity and specific capacitance of PANI nano fibres increased by introducing Cu and Ni ions [165]. Higher electrical conductivity of the cation doped PANI was confirmed from the impedance analysis. The specific capacitance was calculated as 850 F g⁻¹ at 0.86 A g⁻¹ scan rate [179]. Apart from the elevated specific capacitance the metal-doped PANI exhibited good CD cycle stability in comparison to undoped electrode. Supercapacitor properties of un-doped and Mn doped PANI thin films were recorded by depositing on stainless steel substrates through sono-chemical and dip coating method [179]. The doping concentration was varied from 0.4 to 1.6 wt%. Pure PANI was agglomerated and the doping introduced porous nano-fibrous nature to the film. The nano-fibrous had high surface to volume ratio that provided a high CD rate as well as large specific capacitance. As the transition metal ions possess multiple positions for doping, several nitrogen sites of PANI were bound to form inter-chain linkage by coordination. These kinds of interactions (organic-inorganic) were the key factor to prevent the aggregation of PANI [180]. Furthermore, the formation of nano fibrous and porous structure was advantageous for supercapacitor application, due to the reduction of electrode-electrolyte interfacial resistance and facile diffusion of the ions. The intensity of oxidation peak and width of the CV of PANI increased with

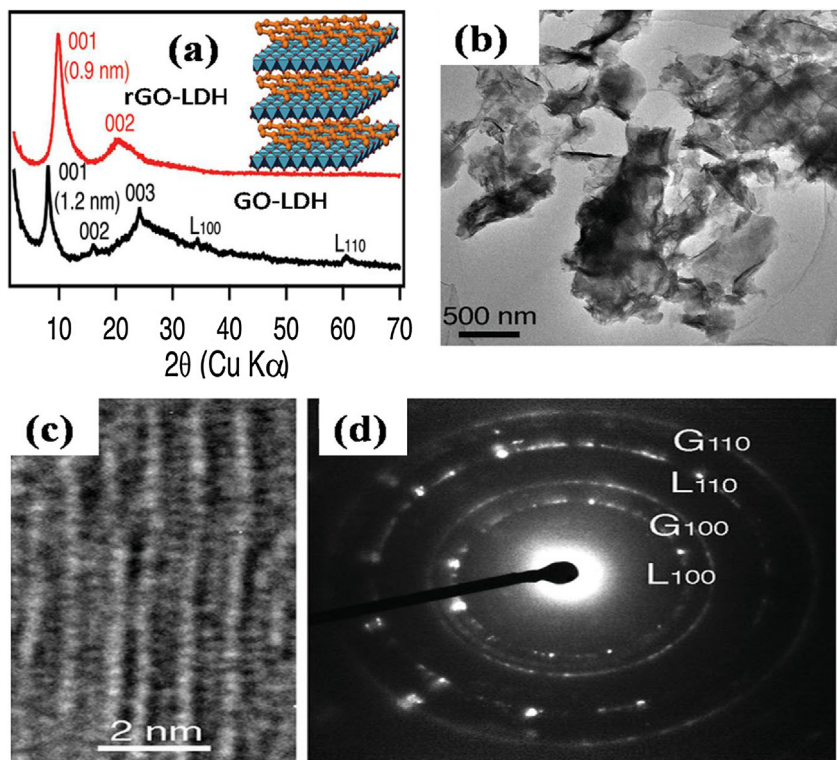


Fig. 14. (a) XRD patterns of GO-LDH and rGO-LDH (b) TEM image, (c) HR-TEM image, and (d) SAED pattern of LDH. Reproduced from Ref. [185] with permission from John Wiley and Sons.

increasing the dopant concentration [180]. The variation of specific capacitance was studied as the function of dopant concentration [180]. Un-doped PANI had a specific capacitance of 285 F g^{-1} while 1.6 Wt% of Mn doped PANI showed high capacitance value of 474 F g^{-1} at the scan rate of 5 mV s^{-1} [178].

Poor cycling stability and low electrical conductivity of PPy can be improved by doping [182–184]. He et al. showed that the supercapacitor properties of the Ru-doped PPy were significantly improved in comparison to the pristine PPy [182]. The current response was successively increased with increasing dopant concentration. It was observed that smaller particle size and homogeneous distribution was achieved due to doping. Ohmic (series resistance) and charge transfer resistance of the doped electrode decreased with increasing Ru content. Ingram and co-workers reported the supercapacitor performance of 'ladder-doped' PPy films [183]. Poly sulfonated aromatic anion doped PPy is effective to achieve rapid insertion/ejection of ions from the electrolyte solution. Hydrophilic ion-conducting channel was formed as the result of doping [183]. The doped PPy showed high areal capacitance of 0.40 F cm^{-2} and high cycling rate in comparison to pristine PPy. On the other hand, structural break down is another major limitation of PPy electrode [183]. Structural break down originated from the CD cycles where counter ion flows repetitively. However, un-doped PPy contained neutral nitrogen group suffered from the irreversible transformation (from neutral to positively charged and vice versa), which started to swell during CD cycles. Huang and co-workers repaired the structural break down through molecular ordering and

doping. The capacitance retention of the modified PPy was recorded as $\sim 86\%$ even after 100,000 CD cycles.

2.4. Superlattice electrode materials

Superlattice is the periodic structure of different materials within nanometer range. Superlattice structures were studied for supercapacitor applications due to the improved electrical conductivity and mobility [185–195]. Generally, superlattice structure consisted of different nano layers where alternate single-layers are sandwiched each other on a molecular scale. As a result quantum tunneling becomes effective providing efficient electron transfer.

Ma et al. reported the direct hetero stacking of transition-metal (Co-Al, Co-Ni) layered double hydroxide (LDH) and GO [171]. Two kinds of charged layers (cationic LDH nanosheets and anionic GO) was sandwiched each other to form heterostructure of superlattice. The charge transfer efficiency was increased due to the formation of alternative layers of LDH and GO. Fig. 14a shows the XRD patterns of LDH nanosheets flocculated with GO (black trace) and rGO (red trace), respectively [185]. It was noticed that the hybridization of LDH with GO generated a basal spacing of 1.2 nm . This thickness was almost equal to the total crystallographic spacing of LDH (0.48 nm) and GO (0.83 nm). The interlayer environment can be modified to achieve high ion diffusion and electron transport. Inset of Fig. 14b shows the schematic illustration of sandwiched LDH nanosheets and graphene. The TEM and HR-TEM images of the LDH/GO

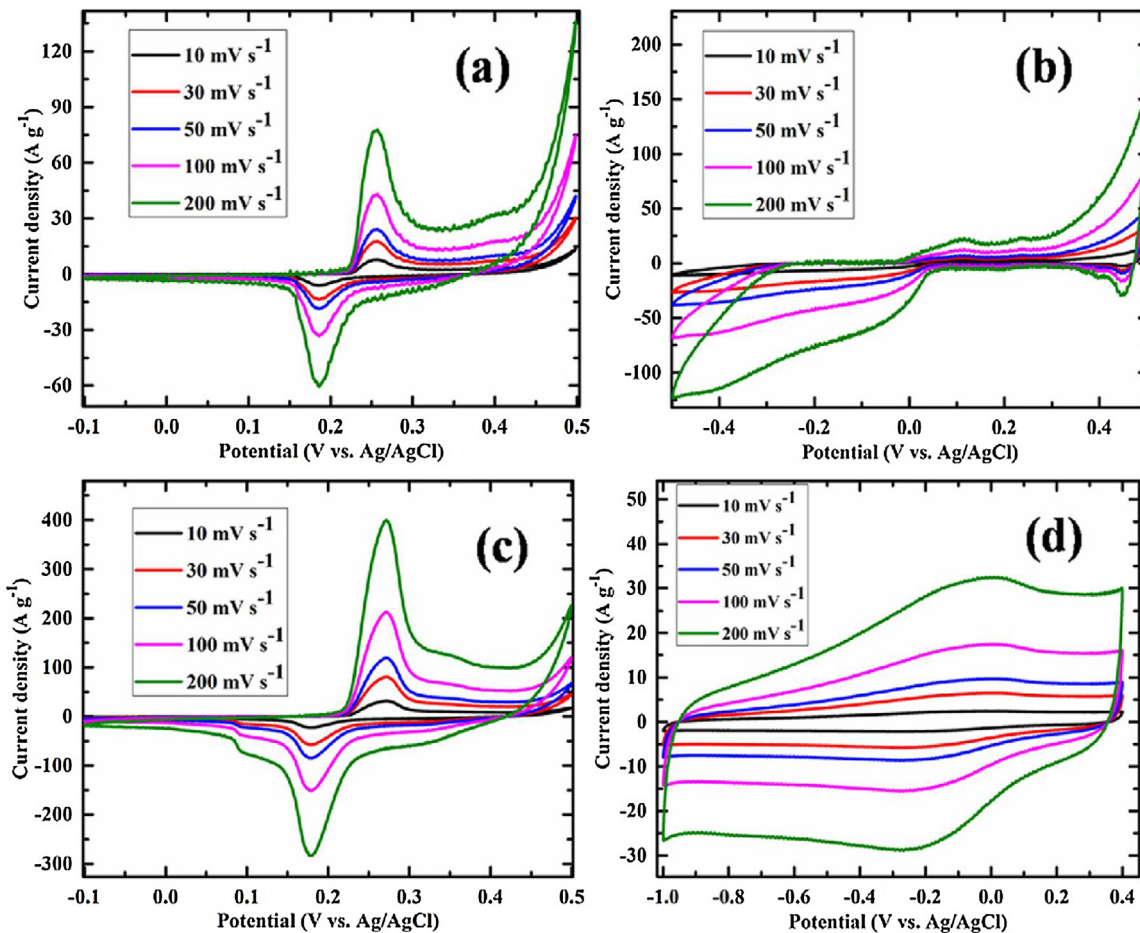


Fig. 15. CV of (a) hBNG1, (b) hBNG2, (c) hBNG3 and (d) hBNG4 at different scan rates.
Reproduced from Ref. [191] with permission from Elsevier.

superlattice are shown in Fig. 14b&c, respectively [185]. The lamellar lattice fringes exhibited different spacing appeared at alternate sequence, suggesting the formation of superlattice structure. The DFT pattern of the LDH/GO superlattice is shown in Fig. 14d [185]. The DFT pattern confirmed the multi layer stacking from the presence of diffraction ring corresponding to both LDH and GO. The formation of superlattice hybridized the EDLC and pseudocapacitance effect generating a high specific capacitance of 650 F g^{-1} [185]. On the other hand, the molecular-scale stacking of electrically conductive graphene with insulating LDH effectively improved the Faradic resistance. As a result, the supercapacitor electrode was able to maintain ideal capacitive CD nature even at 100 Hz establishing its capability for high power applications.

Zhao and co-workers performed the molecular scale hybridization of Co/Ni based LDH and conducting polymer to form superlattice structure [175]. Poly (3, 4-ethylene dioxythiophene): poly (styrene sulfonate) (PEDOT: PSS) was used as the conducting polymer. The organic-inorganic hybridization leads to transfer the benzoid form of the PEDOT chain in to quinoid form (conducting) [189]. As a result, the electrical conductivity of the superlattice was increased as compared to the pure PEDOT:PSS. The electrical conductivity of CoNi-LDH/PEDOT:PSS and pure PEDOT:PSS was measured as 125 and 30 S m^{-1} , respectively [186]. In addition, the homogeneous interface and cherished interaction of the alternate layers ensnared a simultaneous improvement in ion and charge-carrier diffusion as well as high capacitive retention (83.7% retention at 30 A g^{-1}) [175]. The specific capacitance of the LDH/PEDOT:PSS superlattice was measured as 960 F g^{-1} at 2 A g^{-1} current density [189]. The integration of 2D materials raised new opportunity to overcome the limitations of individual materials like low mobility, wide or zero band gap etc. In addition, heterostructure superlattice provided new functionalities coming from the synergistic effect and further can be modified due to the van der Waals interactions.

Nano layer stacking of alternate layer of electrically conducting and non-conducting materials can modify the band structure as well as generate superior redox activity with a backbone of EDLC [190,191]. The modification of electronic band structure of the electrode materials is attractive as it permits the tuning of the electronic properties of the heterostructures. Saha et al. reported the superlattice structure form by stacking of rGO and h-BN layers [191]. Urea, boric acid and GO were used as the source of N, B and rGO/C. Four heterostructure electrode materials (hBNG1, hBNG2, hBNG3 and hBNG4) were synthesized by changing the percentage of precursor materials. Increasing the concentration of rGO within the heterostructure generated various microstructures like C doped h-BN, h-BN/rGO hetero-structure; h-BN/rGO super-lattice and B, N doped rGO, respectively [191]. The content of rGO and h-BN plays a crucial role for the desired structure and electrochemical properties. Position of the conduction and valance band as well as the band gap energy of rGO/h-BN heterostructure was changed with increasing rGO concentration. Fig. 15 shows the CV of different rGO/h-BN heterostructure electrode. The current response and potential window of the CVs change abruptly for different rGO/h-BN microstructure. Highest current response and maximum specific capacitance ($\sim 960 \text{ F g}^{-1}$) was achieved from the electrode (hBNG3), which possesses the superlattice structure [191].

3. Conclusions and outlook

In this review, we have summarized and systematically outlined the conventional strategies associated to the development of heterostructure electrode materials. The electrical conductivity and specific surface area are the major issues for

the high performance supercapacitor. Although, the metal oxides/hydroxides are capable to store huge amount of charge through faradic reaction, poor electrical conductivity are the barrier for practical applications as supercapacitor electrode. On the other hand, metal oxide/hydroxide possesses low surface area and major portion of the active site remain un-used during fast CD process. As a result, capacitance value falls rapidly during the high power applications. Hybridization of binary or ternary metal oxides was established as a use full method because of the creation of defects and facile diffusion path for the electrolyte ions. On the other hand, heterostructure multimetal oxides possess multiple redox activity due to which discharging time of the electrode increases. Conducting polymers showed good supercapacitor properties raised from large π -conjugation, redox and doping/dedoping reactions. However, poor cycle life is one of the major shortcomings for the practical application of conducting polymers is energy storage applications. Hybridization with other electrode materials and doping with cation/anion can overcome these limitations of conducting polymers.

Carbonaceous materials showed characteristic EDLC nature and possess fast CD rate along with high stability and rate capability. However, the specific capacitance of the carbonaceous materials is low in comparison to pseudocapacitance materials. Hybridization of EDLC and pseudocapacitance materials has been studied enormously for the high quality supercapacitor electrode. This kind of hybridization can provide the synergistic advantages of both pseudocapacitance (high specific capacitance) and EDLC (high stability and rate capability) materials. On the other hand, doping of electrode materials was shown an effective way to enhance the electrical conductivity, enlarged the surface area or porosity and enrich the shorten diffusion path for ion transportation. Researchers have shown the effect of heteroatom doping on both the EDLC and pseudocapacitance materials. Doping was also found an effective way to control the structural properties of the electrode material. Furthermore, the electrochemical and structural properties of the superlattice also investigated and it was shown that the periodic arrangement of different kind of materials could overcome many of the shortcomings of the pristine materials. The formation of superlattice generates ion transport in the nano dimension providing superior redox activity. In addition, the superlattice structure consists of EDLC and pseudocapacitance materials showed high capacitance and stability due to good intercalation between the alternate layers.

Although significant advancement has been achieved in the development of electrode materials, there are still obstacles to conquer for better supercapacitor properties. It is essential to develop the heterostructure to meet higher charge storage capability i.e. the energy density along with fast CD capability. There are still several important challenges to be explored in the near future. Synthetically, there are still limitations of electrode preparation without the use of non-conducting additive. Authors considered that the developments of in-situ deposition technique are crucial for the elevated electrochemical performances of heterostructure materials. Functionalization of hybrid nano structure can provide superior structural and electrochemical properties. Significant studies should require exploring the different superlattice structure for supercapacitor application. Insertion of suitable heteroatoms within the binary or ternary metal oxide can provides further improvement of electrochemical properties. Superlattice layers also can be doped with heteroatom for better ion diffusion. However, it is worth to notice that the invalidate effects may also take place due to un-optimized doping. It is expected that intermingle of the different strategy of hybridization of nanomaterials leads to high quality supercapacitors electrodes in the near future.

Acknowledgements

The authors are thankful to the Director of CSIR-CMERI. The authors are also thankful to Council of Scientific and Industrial Research, New Delhi, India for funding Fast Track Translational Project1 (MLP210812).

References

- [1] C. Zhao, W. Zheng, A review for aqueous electrochemical supercapacitors, *Front. Energy Res.* 3 (2015) 1–11.
- [2] G. Yu, X. Xie, L. Pan, Z. Bao, Y. Cui, Hybrid nanostructured materials for high-performance electrochemical capacitors, *Nano Energy* 2 (2013) 213–234.
- [3] G. Wang, L. Zhang, J. Zhang, A review of electrode materials for electrochemical supercapacitors, *Chem. Soc. Rev.* 41 (2012) 797–828.
- [4] V.S. Arunachalam, E.L. Fleischer, The global energy landscape and materials innovation, *MRS Bull.* 33 (2008) 264–288.
- [5] J.P. Holdren, Energy and sustainability, *Science* 315 (2007) 737.
- [6] G. Wang, L. Zhang, J. Zhang, A review of electrode materials for electrochemical supercapacitors, *Chem. Soc. Rev.* 41 (2012) 797–828.
- [7] R.R. Salunkhe, Y. Lee, K. Chang, J. Li, P. Simon, J. Tang, N.L. Torad, C. Hu, Y. Yamauchi, Nanoarchitected graphene-based supercapacitors for next-generation energy-storage applications, *Chem. Eur. J.* 20 (2014) 13838–13852.
- [8] Y. Huang, J. Liang, Y. Chen, An overview of the applications of graphene-based materials in supercapacitors, *Small* 8 (2012) 1805–1834.
- [9] D.P. Dubal, O. Ayyad, V. Ruiz, P. Go'mez-Romero, Hybrid energy storage: the merging of battery and supercapacitor chemistries, *Chem. Soc. Rev.* 44 (2015) 1777–1790.
- [10] X. Yang, L. Zhang, F. Zhang, T. Zhang, Y. Huang, Y. Chen, A high-performance all-solid-state supercapacitor with graphene-doped carbon material electrodes and a graphene oxide-doped ion gel electrolyte, *Carbon* 72 (2014) 381–386.
- [11] V. Khomenko, E. Frackowiak, F. Beguin, Determination of the specific capacitance of conducting polymer/nanotubes composite electrodes using different cell configurations, *Electrochim. Acta* 50 (2005) 2499–2506.
- [12] D.P. Dubal, D. Aradilla, G. Bidan, P. Gentile, T.J.S. Schubert, J. Wimberg, S. Sadki, P. Gomez-Romero, 3D hierarchical assembly of ultrathin MnO₂ nanoflakes on silicon nanowires for high performance micro-supercapacitors in Li-doped ionic liquid, *Sci. Rep.* 5 (2015) 9771.
- [13] O. Koysuren, C. Du, N. Pan, G. Bayram, Preparation and comparison of two electrodes for supercapacitors: pani/cnt/ni and pani/alizarin-treated nickel, *J. Appl. Polym. Sci.* 113 (2009) 1070–1081.
- [14] Y. Shao, M.F. El-Kady, L.J. Wang, Q. Zhang, Y. Li, H. Wang, M.F. Mousavina, R.B. Kaner, Graphene-based materials for flexible supercapacitors, *Chem. Soc. Rev.* 44 (2015) 3639–3665.
- [15] C. Hu, L. Song, Z. Zhang, N. Chen, Z. Feng, L. Qu, Tailored graphene systems for unconventional applications in energy conversion and storage devices, *Energy Environ. Sci.* 8 (2015) 31–54.
- [16] A. Reddy, A. Srivastava, S. Gowda, H. Gullapalli, M. Dubey, P.M. Ajayan, Synthesis of nitrogen-doped graphene films for lithium battery application, *ACS Nano* 4 (2010) 6337–6342.
- [17] H.M. Jeong, J.W. Lee, W.H. Shin, Y.J. Choi, H.J. Shin, J.K. Kang, J.W. Choi, Nitrogen doped graphene for high-performance ultracapacitors and the importance of nitrogen-doped sites at basal planes, *Nano Lett.* 11 (2011) 2472–2477.
- [18] L.T. Qu, Y. Liu, J.B. Baek, L.M. Dai, Nitrogen-doped graphene as efficient metal-free electrocatalyst for oxygen reduction in fuel cells, *ACS Nano* 4 (2010) 1321–1326.
- [19] H. Zhang, X. Lv, Y. Li, Y. Wang, J. Li, P25-Graphene composite as a high performance photocatalyst, *ACS Nano* 4 (2010) 380–386.
- [20] Z. Yu, L. Tetard, L. Zhai, J. Thomas, Supercapacitor electrode materials: nanostructures from 0 to 3 dimensions, *Energy Environ. Sci.* 8 (2015) 702–730.
- [21] Y. Zhang, L. Li, H. Su, W. Huang, X. Dong, Binary metal oxide: advanced energy storage materials in supercapacitors, *J. Mater. Chem. A* 3 (2015) 43–59.
- [22] D. Chen, Q. Wang, R. Wang, G. Shen, Ternary oxide nanostructured materials for supercapacitors: a review, *J. Mater. Chem. A* 3 (2015) 10158–10173.
- [23] Q.F. Wang, B. Liu, X.F. Wang, S.H. Ran, L.M. Wang, D. Chen, G.Z. Shen, Morphology evolution of urchin-like NiCo₂O₄ nanostructures and their applications as pseudocapacitors and photoelectrochemical cells, *J. Mater. Chem.* 22 (2012) 21647–21653.
- [24] S.K. Chang, K.T. Lee, Z. Zainal, K.B. Tan, N.A. Yusof, W.M.D.W. Yusoff, J.F. Lee, N. L. Wu, Structural and electrochemical properties of manganese substituted nickel cobaltite for supercapacitor application, *Electrochim. Acta* 67 (2012) 67–72.
- [25] X. Liu, S. Shi, Q. Xiong, L. Li, Y.J. Zhang, H. Tang, C.D. Gu, X.L. Wang, J.P. Tu, Hierarchical NiCo₂O₄@NiCo₂O₄ core/shell nanoflake arrays as high-performance supercapacitor materials, *ACS Appl. Mater. Interfaces* 5 (2013) 8790–8795.
- [26] C. Yuan, J. Li, L. Hou, L. Yang, L. Shen, X. Zhang, Facile template-free synthesis of ultralayered mesoporous nickel cobaltite nanowires towards high-performance electrochemical capacitors, *J. Mater. Chem.* 22 (2012) 16084–16090.
- [27] H. Jiang, J. Ma, C. Li, Hierarchical porous NiCo₂O₄ nanowires for high-rate supercapacitors, *Chem. Commun.* 48 (2012) 4465–4467.
- [28] P. Lavela, J.L. Tirado, CoFe₂O₄ and NiFe₂O₄ synthesized by sol-gel procedures for their use as anode materials for Li ion batteries, *J. Power Sources* 172 (2007) 379–387.
- [29] D. Guo, H. Zhang, X. Yu, M. Zhang, P. Zhang, Q. Li, T. Wang, Facile synthesis and excellent electrochemical properties of CoMoO₄ nanoplate arrays as supercapacitors, *J. Mater. Chem. A* 1 (2013) 7247–7254.
- [30] M. Liu, L. Kong, X. Ma, C. Lu, X. Li, Y. Luo, L. Kang, Hydrothermal process for the fabrication of CoMoO₄·0.9H₂O nanorods with excellent electrochemical behaviour, *New J. Chem.* 36 (2012) 1713–1716.
- [31] L. Zhang, H. Gong, Partial conversion of current collector into nickel copper oxide electrode materials for high performance energy storage device, *ACS Appl. Mater. Interfaces* 7 (2015) 15277–15284.
- [32] J. Zhang, F. Liu, J.P. Cheng, X.B. Zhang, Binary nickel-cobalt oxides electrode materials for high-performance supercapacitors: influence of its composition and porous nature, *ACS Appl. Mater. Interfaces* 7 (2015) 17630–17640.
- [33] S. Saha, S. Chhetri, P. Khanra, P. Samanta, H. Koo, N.C. Murmu, T. Kuila, In-situ hydrothermal synthesis of MnO₂/NiO@Ni hetero structure electrode for hydrogen evolution reaction and high energy asymmetric supercapacitor applications, *J. Energy Storage* 6 (2016) 22–31.
- [34] L. Li, Y. Zhang, F. Shi, Y. Zhang, J. Zhang, C. Gu, X. Wang, J. Tu, Spinel manganese-nickel-cobalt ternary oxide nanowire array for high-performance electrochemical capacitor applications, *ACS Appl. Mater. Interfaces* 6 (2014) 18040–18047.
- [35] D. Cai, B. Liu, D. Wang, L. Wang, Y. Liu, H. Li, Y. Wang, Q. Li, T. Wang, Construction of unique NiCo₂O₄ nanowire@CoMoO₄ nanoplate core/shell arrays on Ni foam for high areal capacitance supercapacitors, *J. Mater. Chem. A* 2 (2014) 4954–4960.
- [36] D. Du, R. Lan, W. Xu, R. Beanland, H. Wang, S. Tao, Preparation of a hybrid Cu₂O/CuMoO₄ nanosheet electrode for high-performance asymmetric supercapacitors, *J. Mater. Chem. A* 4 (2016) 17749–17756.
- [37] J. Zhu, Z. Xu, B. Lu, Ultrafine Au nanoparticles decorated NiCo₂O₄ nanotubes as anode material for high-performance supercapacitor and lithium-ion battery applications, *Nano Energy* 7 (2014) 114–123.
- [38] W. Yang, Z. Gao, J. Ma, X. Zhang, J. Wang, J. Liu, Hierarchical NiCo₂O₄@NiO core–shell heterostructured nanowire arrays on carbon cloth for a high-performance flexible all-solid-state electrochemical capacitor, *J. Mater. Chem. A* 2 (2014) 1448–1457.
- [39] K. Xu, W. Li, Q. Liu, B. Li, X. Liu, L. An, Z. Chen, R. Zou, J. Hu, Hierarchical mesoporous NiCo₂O₄@MnO₂ core–shell nanowire arrays on nickel foam for aqueous asymmetric supercapacitors, *J. Mater. Chem. A* 2 (2014) 4795–4802.
- [40] B. Li, P. Gu, Y. Feng, G. Zhang, K. Huang, H. Xue, H. Pang, Ultrathin Nickel-Cobalt Phosphate 2D nanosheets for electrochemical energy storage under aqueous/solid-state electrolyte, *Adv. Funct. Mater.* 27 (2017) 1605784.
- [41] H. Pang, X. Li, Q. Zhao, H. Xue, W. Lai, Z. Hu, W. Huang, One-pot synthesis of heterogeneous Co₃O₄-nanocube/Co(OH)₂-nanosheet hybrids for high-performance flexible asymmetric all-solid-state supercapacitors, *Nano Energy* 35 (2017) 138–145.
- [42] S. Sahoo, T.T. Nguyen, J. Shim, Mesoporous Fe-Ni-Co ternary oxide nanoflake arrays on Ni foam for high-performance supercapacitor applications, *J. Ind. Eng. Chem.* (2018), doi:<http://dx.doi.org/10.1016/j.jiec.2018.02.014>.
- [43] C. Wu, J. Cai, Q. Zhang, X. Zhou, Y. Zhu, P. Shen, K. Zhang, Hierarchical mesoporous Zinc-Nickel-Cobalt ternary oxide nanowire arrays on nickel foam as high performance electrodes for supercapacitors, *ACS Appl. Mater. Interfaces* 7 (2015) 26512–26521.
- [44] X. Li, L. Wang, J. Shi, N. Du, G. He, Multishelled Nickel-Cobalt oxide hollow microspheres with optimized compositions and shell porosity for high-performance pseudocapacitors, *ACS Appl. Mater. Interfaces* 8 (2016) 17276–17283.
- [45] Y. Lu, B. Li, S. Zheng, Y. Xu, H. Xue, H. Pang, Syntheses and energy storage applications of MxSy (M = Cu, Ag, Au) and their composites: rechargeable batteries and supercapacitors, *Adv. Funct. Mater.* 27 (2017) 1703949.
- [46] S. Zheng, H. Xue, H. Pang, Supercapacitors based on metal coordination materials, *Coord. Chem. Rev.* (2018), doi:<http://dx.doi.org/10.1016/j.ccr.2017.07.002>.
- [47] J. Zhang, P. Gu, J. Xu, H. Xue, H. Pang, High performance of electrochemical lithium storage batteries: ZnO-based nanomaterials for lithium-ion and lithium-sulfur batteries, *Nanoscale* 8 (2016) 18578–18595.
- [48] Y. Wang, J. Guo, T. Wang, J. Shao, D. Wang, Y. Yang, Mesoporous transition metal oxides for supercapacitors, *Nanomaterial* 5 (2015) 1667–1689.
- [49] J. Kim, H. Ju, A.I. Inamdar, Y. Jo, J. Han, H. Kim, H. Im, Synthesis and enhanced electrochemical supercapacitor properties of Ag-MnO₂-polyaniline nanocomposite electrodes, *Energy* 70 (2014) 473–477.
- [50] S. Radhakrishnan, S. Prakash, Chepuri R.K. Rao, M. Vijayan, Organically soluble bifunctional polyaniline–magnetite composites for sensing and supercapacitor applications, *Electrochim. Solid-State Lett.* 12 (2009) A84–A87.
- [51] Q. Wu, M. Chen, K. Chen, S. Wang, C. Wang, G. Diao, Fe₃O₄-based core/shell nanocomposites for high-performance electrochemical supercapacitors, *J. Mater. Sci.* 51 (2016) 1572–1580.

- [52] P.M. Kharade, S.G. Chavan, D.J. Salunkhe, P.B. Joshi, S.M. Mane, S.B. Kulkarni, Synthesis and characterization of PANI/MnO₂ bi-layered electrode and its electrochemical supercapacitor properties, *Mater. Res. Bull.* 52 (2014) 37–41.
- [53] Jaidev, R.I. Jafri, A.K. Mishra, S. Ramaprabhu, Polyaniline-MnO₂ nanotube hybrid nanocomposite as supercapacitor electrode material in acidic electrolyte, *J. Mater. Chem.* 21 (2011) 17601–17605.
- [54] T. Liu, G. Shao, M. Ji, G. Wang, Polyaniline/MnO₂ composite with high performance as supercapacitor electrode via pulse electrodeposition, *Polym. Compos.* 36 (2015) 113–120.
- [55] H. Xu, J. Wu, Y. Chen, J. Zhang, B. Zhang, Facile synthesis of polyaniline/NiCo₂O₄ nanocomposites with enhanced electrochemical properties for supercapacitors, *Ionics* 21 (2015) 2615–2622.
- [56] S. Faraji, F.N. Ani, The development supercapacitor from activated carbon by electroless plating-a review, *Renew. Sustain. Energy Rev.* 42 (2015) 823–834.
- [57] Z. Chen, D. Yu, W. Xiong, P. Liu, Y. Liu, L. Dai, Graphene-based nanowire supercapacitors, *Langmuir* 30 (2014) 3567–3571.
- [58] T. Pandolfo, V. Ruiz, S. Sivakkumar, J. Nerkar, *Supercapacitors: Materials, Systems and Applications*, Wiley-VCH Verlag GmbH & Co KgaA, Weinheim, Germany, 2013, pp. 69–109.
- [59] J. Hou, C. Cao, F. Idrees, X. Ma, Hierarchical porous nitrogen-doped carbon nanosheets derived from silk for ultrahigh-capacity battery anodes and supercapacitors, *ACS Nano* 9 (2015) 2556–2564.
- [60] Y. Li, J. Dong, J. Zhang, X. Zhao, P. Yu, L. Jin, Q. Zhang, Nitrogen-doped carbon membrane derived from polyimide as free-standing electrodes for flexible supercapacitors, *Small* 11 (2015) 3476–3484.
- [61] T. Chen, H. Peng, M. Durstock, L. Da, High-performance transparent and stretchable all-solid supercapacitors based on highly aligned carbon nanotube sheets, *Sci. Rep.* 4 (2014) 3612.
- [62] K. Chen, Y. Yang, K. Li, Z. Ma, Y. Zhou, D. Xue, CoCl₂ designed as excellent pseudocapacitor electrode materials, *ACS Sustain. Chem. Eng.* 2 (2014) 440–444.
- [63] W. Chen, R.B. Rakhi, H.N. Alshareef, Morphology-dependent enhancement of the pseudocapacitance of template-guided tunable polyaniline nanostructures, *J. Phys. Chem. C* 117 (2013) 15009–15019.
- [64] M. Shao, Z. Li, R. Zhang, F. Ning, M. Wei, D.G. Evans, X. Duan, Hierarchical conducting polymer@clay core-shell arrays for flexible all-solid-state supercapacitor devices, *Small* 11 (2015) 3530–3538.
- [65] S. Nejati, T.E. Minford, Y.Y. Smolin, K.K.S. Lau, Enhanced charge storage of ultrathin polythiophene films within porous nanostructures, *ACS Nano* 8 (2014) 5413–5422.
- [66] Y. Lin, X. Wang, G. Qian, J.J. Watkins, Additive-driven self-assembly of well-ordered mesoporous carbon/iron oxide nanoparticle composites for supercapacitors, *Chem. Mater.* 26 (2014) 2128–2137.
- [67] S. Yang, X. Song, P. Zhang, J. Sun, L. Gao, Self-assembled α -Fe₂O₃ mesocrystals/graphene nanohybrid for enhanced electrochemical capacitors, *Small* 10 (2014) 2270–2279.
- [68] A.M. Khattak, H. Yin, Z.A. Ghazi, B. Liang, A. Iqbal, N.A. Khan, Y. Gao, L. Li, Z. Tang, Three dimensional iron oxide/graphene aerogel hybrids as all-solid-state flexible supercapacitor electrodes, *RSC Adv.* 6 (2016) 58994–59000.
- [69] K.K. Lee, S. Deng, H.M. Fan, S. Mhaisalkar, H.R. Tan, E.S. Tok, K.P. Loh, W.S. Chin, C.H. Sow, α -Fe2O3 nanotubes-reduced graphene oxide composites as synergistic electrochemical capacitor materials, *Nanoscale* 4 (2012) 2958–2961.
- [70] Z. Song, W. Liu, P. Xiao, Z. Zhao, G.g. Liu, J. Qiu, Nano-iron oxide (Fe₂O₃)/three-dimensional graphene aerogel composite as supercapacitor electrode materials with extremely wide working potential window, *Mater. Lett.* 145 (2015) 44–47.
- [71] S. Ghasemi, F. Ahmadi, Effect of surfactant on the electrochemical performance of graphene/iron oxide electrode for supercapacitor, *J. Power Sources* 289 (2015) 129–137.
- [72] A. Vu, X. Li, J. Phillips, A. Han, W.H. Smyrl, P. Bühlmann, A. Stein, Three-dimensionally ordered mesoporous (3DOM) carbon materials as electrodes for electrochemical double-layer capacitors with ionic liquid electrolytes, *Chem. Mater.* 25 (2013) 4137–4148.
- [73] A.B. Fuertes, M. Sevilla, Hierarchical microporous/mesoporous carbon nanosheets for high-performance supercapacitors, *ACS Appl. Mater. Interfaces* 7 (2015) 4344–4353.
- [74] B. You, J. Jiang, S. Fan, Three-dimensional hierarchically porous all-carbon foams for supercapacitor, *ACS Appl. Mater. Interfaces* 6 (2014) 15302–15308.
- [75] Z. Qin, M. Taylor, M. Hwang, K. Bertoldi, M.J. Buehler, Effect of wrinkles on the surface area of graphene: toward the design of nanoelectronics, *Nano Lett.* 14 (2014) 6520–6525.
- [76] X. Chen, L. Qiu, J. Ren, G. Guan, H. Lin, Z. Zhang, P. Chen, Y. Wang, H. Peng, Novel electric double-layer capacitor with a coaxial fiber structure, *Adv. Mater.* 25 (2013) 6436–6441.
- [77] D. Krishnan, K. Raidongia, J. Shao, J. Huang, Graphene oxide assisted hydrothermal carbonization of carbon hydrates, *ACS Nano* 8 (2014) 449–457.
- [78] L. Deng, R.J. Young, I.A. Kinloch, A.M. Abdelkader, S.M. Holmes, D.A.D.H. Rio, S. J. Eichhorn, Supercapacitance from cellulose and carbon nanotube nanocomposite fibers, *ACS Appl. Mater. Interfaces* 5 (2013) 9983–9990.
- [79] E. Wilson, M.F. Islam, Ultracompressible, high-rate supercapacitors from graphene-coated carbon nanotube aerogels, *ACS Appl. Mater. Interfaces* 7 (2015) 5612–5618.
- [80] O.S. Kwon, T. Kim, J.S. Lee, S.J. Park, H. Park, M. Kang, J.E. Lee, J. Jang, H. Yoon, Fabrication of graphene sheets intercalated with manganese oxide/carbon nanofibers: toward highcapacity energy storage, *Small* 9 (2013) 248–254.
- [81] Y. Bu, S. Wang, H. Jin, W. Zhang, J. Lin, J. Wang, Synthesis of porous NiO/reduced graphene oxide composites for supercapacitors, *J. Electrochem. Soc.* 159 (2012) A990–A994.
- [82] G. Cai, J. Tu, J. Zhang, Y. Mai, Y. Lu, C. Gua, X. Wang, An efficient route to a porous NiO/reduced graphene oxide hybrid film with highly improved electrochromic properties, *Nanoscale* 4 (2012) 5724–5730.
- [83] W. Li, Y. Bu, H. Jin, J. Wang, W. Zhang, S. Wang, J. Wang, The preparation of hierarchical flower like nio/reduced graphene oxide composites for high performance supercapacitor applications, *Energ. Fuels* 27 (2013) 6304–6310.
- [84] B. Zhao, J. Song, P. Liu, W. Xu, T. Fang, Z. Jiao, H. Zhang, Y. Jiang, Monolayer graphene/NiO nanosheets with two-dimension structure for supercapacitors, *J. Mater. Chem.* 21 (2011) 18792–18798.
- [85] K. Ling, A. Chen, L. He, W. Wang, Nickel oxide as an electrode material for supercapacitor, *J. Mater. Sci. Technol.* 4 (2002) 383–384.
- [86] K.C. Liu, M.A. Anderson, Porous nickel oxide/nickel films for electrochemical capacitors, *J. Electrochem. Soc.* 143 (1996) 124–130.
- [87] V. Srinivasan, J.W. Weidner, Studies on the capacitance of nickel oxide films: effect of heatingtemperature and electrolyte concentration, *J. Electrochem. Soc.* 147 (2000) 880–885.
- [88] C. Ge, Z. Hou, B. He, F. Zeng, J. Cao, Y. Liu, Y. Kuang, Three-dimensional flower-like nickel oxide supported on graphenesheets as electrode material for supercapacitors, *J. Sol-Gel Sci. Technol.* 63 (2012) 146–152.
- [89] B. Gao, C. Yuan, L. Su, L. Chen, X. Zhang, Nickel oxide coated on ultrasonically pretreated carbonanotubes for supercapacitor, *J. Solid State Electrochem.* 13 (2009) 1251–1257.
- [90] B. Yuan, C. Xu, D. Deng, Y. Xing, L. Liu, H. Pang, D. Zhang, Graphene oxide/nickel oxide modified glassy carbon electrode for supercapacitorand nonenzymatic glucose sensor, *Electrochim. Acta* 88 (2013) 708–712.
- [91] P. Lin, Q. She, B. Hong, X. Liu, Y. Shi, Z. Shi, M. Zheng, Q. Dong, The nickel oxide/CNT composites with high capacitance for supercapacitor, *J. Electrochem. Soc.* 157 (2010) A818–A823.
- [92] J. Yan, Z. Fan, W. Sun, G. Ning, T. Wei, Q. Zhang, R. Zhang, L. Zhi, F. Wei, Advanced asymmetric supercapacitors based on Ni(OH)₂/Graphene and porous graphene electrodes with highenergy density, *Adv. Funct. Mater.* 22 (2012) 2632–2641.
- [93] H. Wang, H.S. Casalongue, Y. Liang, H. Dai, Ni(OH)₂ nanoplates grown on graphene as advancedelectrochemical pseudocapacitor materials, *J. Am. Chem. Soc.* 132 (2010) 7472–7477.
- [94] Y. Tang, Y. Liu, W. Guo, T. Chen, H. Wang, S. Yu, F. Gao, Highly oxidized graphene anchored Ni(OH)₂ nanoflakesas pseudocapacitor materials for ultrahigh loadingelectrode with high areal specific capacitance, *J. Phys. Chem. C* 118 (2014) 24866–24876.
- [95] J. Yan, Z. Fan, T. Wei, W. Qian, M. Zhang, F. Wei, Fast and reversible surface redox reaction of graphene-MnO₂composites as supercapacitor electrodes, *Carbon* 48 (2010) 3825–3833.
- [96] Z. Li, Y. Mi, X. Liu, S. Liu, S. Yang, J. Wan, Flexible graphene/MnO₂ composite papers for supercapacitor electrodes, *J. Mater. Chem.* 21 (2011) 14706–14711.
- [97] M. Lee, C. Fan, Y. Wang, H. Li, J. Chang, C. Tseng, Improved supercapacitor performance of MnO₂-graphene composites constructed using a supercriticalfluid and wrapped with an ionic liquid, *J. Mater. Chem. A* 1 (2013) 3395–3405.
- [98] Z. Zhang, F. Xiao, L. Qian, J. Xiao, S. Wang, Y. Liu, Facile Synthesis of 3D MnO₂-graphene and carbon nanotube-graphene composite networks for highperformance, flexible, all-solid-state asymmetricsupercapacitors, *Adv. Energy Mater.* 4 (2014) 1400064.
- [99] Z. Fan, J. Yan, T. Wei, L. Zhi, G. Ning, T. Li, F. Wei, Asymmetric supercapacitors based on graphene/MnO₂and activated carbon nanofiber electrodes with highpower and energy density, *Adv. Funct. Mater.* 21 (2011) 2366–2375.
- [100] S. Chen, J. Zhu, X. Wu, Q. Han, X. Wang, Graphene oxideMnO₂nanocomposites for supercapacitors, *ACS Nano* 4 (2010) 2822–2830.
- [101] Z. Wu, W. Ren, D. Wang, F. Li, B. Liu, H. Cheng, High-energy MnO₂ nanowire/graphene and graphene asymmetricelectrochemical capacitors, *ACS Nano* 4 (2010) 5835–5842.
- [102] J. Chang, M. Jin, F. Yao, T.H. Kim, V.T. Le, H. Yue, F. Gunes, B. Li, A. Ghosh, S. Xie, Y.H. Lee, Asymmetric supercapacitors based on graphene/MnO₂ nanospheres and graphene/MoO₃ nanosheets with highenergy density, *Adv. Funct. Mater.* 23 (2013) 5074–5083.
- [103] L. Peng, X. Peng, B. Liu, C. Wu, Y. Xie, G. Yu, Ultrathin two-dimensional MnO₂/Graphene hybrid nanostructuresfor high-performance, flexible planar supercapacitors, *Nano Lett.* 13 (2013) 2151–2157.
- [104] M. Jana, S. Saha, P. Samanta, N.C. Murmu, N.H. Kim, T. Kuila, J.H. Lee, A successive ionic layer adsorption and reaction (SILAR) method to fabricate a layer-by-layer (LBL) MnO₂-reduced graphene oxideassembly for supercapacitor application, *J. Power Sources* 340 (2017) 380–392.
- [105] J. Xia, L. Gao, J. Cao, W. Wang, Z. Chen, Preparation and electrochemical capacitance of cobalt oxide (Co₃O₄) nanotubes as supercapacitor material, *Electrochim. Acta* 56 (2010) 732–736.
- [106] J.P. Cheng, X. Chen, J.S. Wu, F. Liu, X.B. Zhang, V.P. Dravid, Porous cobalt oxides with tunable hierarchical morphologies for supercapacitor electrodes, *CrystEngComm* 14 (2012) 6702–6709.
- [107] C. Xiang, M. Li, M. Zhi, A. Manivannan, N. Wu, A reduced graphene oxide/Co₃O₄ composite for supercapacitor electrode, *J. Power Sources* 226 (2013) 65–70.
- [108] W. Zhou, J. Liu, T. Chen, K.S. Tan, X. Jia, Z. Luo, C. Cong, H. Yang, C.M. Li, T. Yu, Fabrication of Co₃O₄-reduced graphene oxide scrolls forhigh-performance supercapacitor electrodes, *Phys. Chem. Chem. Phys.* 13 (2011) 14462–14465.

- [109] X.C. Dong, H. Xu, X.W. Wang, Y.X. Huang, M.B. C-Park, H. Zhang, L.H. Wang, W. Huang, P. Chen, 3D graphenecobalt oxide electrodefor high-performance supercapacitorand enzymeless glucose detection, *ACS Nano* 6 (2012) 206–3213.
- [110] S. Park, S. Kim, Effect of carbon blacks filler addition on electrochemical behaviors of Co_3O_4 /graphene nanosheets as a supercapacitor electrode, *Electrochim. Acta* 89 (2013) 516–522.
- [111] W. Bi, G. Gao, Y. Wu, H. Yang, J. Wang, Y. Zhang, X. Liang, Y. Liu, G. Wu, Novel three-dimensional island-chain structured V_2O_5 /graphene/MWCNT hybrid aerogels for supercapacitors with ultralong cycle life, *RSC Adv.* 7 (2017) 7179–7187.
- [112] N.H.N. Azman, M.S. Mamat, L.H. Ngee, Y. Sulaiman, Graphene-based ternary composites for supercapacitors, *Int. J. Energy Res.* (2018), doi:<http://dx.doi.org/10.1002/er.4001>.
- [113] G. Wee, H.Z. Soh, Y.L. Cheah, S.G. Mhaisalkar, M. Srinivasan, Synthesis and electrochemical properties of electrospun V_2O_5 nanofibers as supercapacitor electrodes, *J. Mater. Chem.* 20 (2010) 6720–6725.
- [114] H.Y. Lee, J.B. Goodenough, Ideal supercapacitor behavior of amorphous $\text{V}_2\text{O}_5 \cdot \text{nH}_2\text{O}$ in potassiumchloride (KCl) aqueous solution, *J. Solid State Chem.* 148 (1999) 81–84.
- [115] H. Yoon, M. Choi, K.J. Lee, J. Jang, Versatile strategies for fabricating polymer nanomaterials with controlled size and morphology, *Macromol. Res.* 16 (2008) 85–102.
- [116] Z. Wang, X. He, S. Ye, Y. Tong, G. Li, Design of polypyrrole/polyaniline double-walled nanotube arrays for electrochemical energy storage, *ACS Appl. Mater. Interfaces* 6 (2014) 642–647.
- [117] H. Park, T. Kim, J. Huh, M. Kang, J.E. Lee, H. Yoon, Anisotropic growth control of polyaniline nanostructures and their morphology-dependent electrochemical characteristics, *ACS Nano* 6 (2012) 7624–7633.
- [118] M.R. Arcila-Velez, M.E. Roberts, Redox solute doped polypyrrole for high-charge capacity polymer electrodes, *Chem. Mater.* 26 (2014) 1601–1607.
- [119] H. Gómez, M.K. Ramb, F. Alvia, P. Villalba, E. Stefanakosc, A. Kumara, Graphene-conducting polymer nanocomposite as novel electrode for supercapacitors, *J. Power Sources* 196 (2011) 4102–4108.
- [120] W. Fan, C. Zhang, W.W. Tjiu, K.P. Pramoda, C. He, T. Liu, Graphene-wrapped polyaniline hollow spheres as novel hybrid electrode materials for supercapacitor applications, *ACS Appl. Mater. Interfaces* 5 (2013) 3382–3391.
- [121] X. Feng, R. Li, Y. Ma, R. Chen, N. Shi, Q. Fan, W. Huang, One-Step electrochemical synthesis of graphene/polyaniline composite film and its applications, *Adv. Funct. Mater.* 21 (2011) 2989–2996.
- [122] J. Yana, T. Weia, Z. Fana, W. Qianb, M. Zhang, X. Shena, F. Weib, Preparation of graphene nanosheet/carbon nanotube/polyaniline composite as electrode material for supercapacitors, *J. Power Sources* 195 (2010) 3041–3045.
- [123] Z. Li, H. Zhang, Q. Liu, L. Sun, L. Stanciu, J. Xie, Fabrication of high-surface-area graphene/polyaniline nanocomposites and their application in supercapacitors, *ACS Appl. Mater. Interfaces* 5 (2013) 2685–2691.
- [124] E. Coskun, E.A. Zaragoza-Contreras, H.J. Salavagione, Synthesis of sulfonated graphene/polyaniline composites with improved electroactivity, *Carbon* 50 (2012) 2235–2243.
- [125] S. Wang, L. Ma, M. Gan, S. Fu, W. Dai, T. Zhou, X. Sun, H. Wang, H. Wang, Free-standing 3D graphene/polyaniline composite film electrodes for high-performance supercapacitors, *J. Power Sources* 299 (2015) 347–355.
- [126] S. Li, C. Zhao, K. Shu, C. Wang, Z. Guo, Mechanically strong high performance layered polypyrrole nano fibre/graphene film for flexible solid state supercapacitor, *Carbon* 79 (2014) 554–562.
- [127] C. Zhao, K. Shu, C. Wang, S. Gambhir, G.G. Wallace, Reduced graphene oxide and polypyrrole/reduced graphene oxide composite coated stretchable fabric electrodes for supercapacitor application, *Electrochim. Acta* 172 (2015) 15–19.
- [128] J. Xu, D. Wang, Y. Yuan, W. Wei, L. Duan, L. Wang, H. Bao, W. Xu, Polypyrrole/ reduced graphene oxide coated fabric electrodes for supercapacitor application, *Org. Electron.* 24 (2015) 153–159.
- [129] D. Yu, Q. Qian, L. Wei, W. Jiang, K. Goh, J. Wei, J. Zhang, Y. Chen, Emergence of fiber supercapacitors, *Chem. Soc. Rev.* 44 (2015) 647–662.
- [130] J. Zhu, Y. Xu, J. Wang, J. Lin, X. Sun, S. Mao, The effect of various electrolyte cations on electrochemical performance of polypyrrole/RGO based supercapacitors, *Phys. Chem. Chem. Phys.* 17 (2015) 28666–28673.
- [131] Y. Chen, M. Han, Y. Tang, J. Bao, S. Li, Y. Lan, Z. Dai, Polypyrrole-polyoxometalate/reduced graphene oxide ternary nanohybrids for flexible, all-solid-state supercapacitors, *Chem. Commun.* 51 (2015) 12377–12380.
- [132] L. Lai, L. Wang, H. Yang, N.G. Sahoo, Q.X. Tam, J. Liu, C.K. Poh, S.H. Lim, Z. Shen, J. Lin, Tuning graphene surface chemistry to prepare graphene/polypyrrole supercapacitors with improved performance, *Nano Energy* 1 (2012) 723–731.
- [133] A. Davies, P. Audette, B. Farrow, F. Hassan, Z. Chen, J. Choi, A. Yu, Graphene-based flexible supercapacitors: pulse-electropolymerization of polypyrrole on free-standing graphene films, *J. Phys. Chem. C* 115 (2011) 17612–17620.
- [134] Y. Li, J. Dong, J. Zhang, X. Zhao, P. Yu, L. Jin, Q. Zhang, Nitrogen-doped carbon membrane derived from polyimide as free-standing electrodes for flexible supercapacitors, *Small* 11 (2015) 3476–3484.
- [135] X.Y. Chen, C. Chen, Z.J. Zhang, D.H. Xie, X. Deng, Nitrogen-doped porous carbon prepared from urea formaldehyde resins by template carbonization method for supercapacitors, *Ind. Eng. Chem. Res.* 52 (2013) 10181–10188.
- [136] X.Y. Chen, C. Chen, Z.J. Zhang, D.H. Xie, Nitrogen-doped porous carbon spheres derived from polyacrylamide, *Ind. Eng. Chem. Res.* 52 (2013) 12025–12031.
- [137] H. Peng, G. Ma, K. Sun, J. Mu, Z. Zhang, Z. Lei, Facile synthesis of poly(p-phenylenediamine)- derived three-dimensional porous nitrogen-doped carbon networks for high performance supercapacitors, *J. Phys. Chem. C* 118 (2014) 29507–29516.
- [138] Y. Deng, Y. Xie, K. Zoua, X. Ji, Review on recent advances in nitrogen-doped carbons: preparations and applications in supercapacitors, *J. Mater. Chem. A* 4 (2016) 1144–1173.
- [139] W. Sugimoto, T. Shibutani, Y. Murakami, Y. Takasu, Charge storage capabilities of rutile-type $\text{RuO}_2\text{-VO}_2$ solid solution for electrochemical supercapacitors, *Solid-State Lett.* 5 (2002) A170–A172.
- [140] J. Duan, S. Chen, M. Jaroniec, S.Z. Qiao, Heteroatom-doped graphene-based materials for energy-relevant electrocatalytic processes, *ACS Catal.* 5 (2015) 5207–5234.
- [141] Y.F. Nie, Q. Wang, X.Y. Chen, Z.J. Zhang, Nitrogen and oxygen functionalized hollow carbon materials: the capacitive enhancement by simply incorporating novel redox additives into H_2SO_4 electrolyte, *J. Power Sources* 320 (2016) 140–152.
- [142] D. Xu, W. Hu, X.N. Sun, P. Cui, X.Y. Chen, Redox additives of Na_2MoO_4 and KI: Synergistic effect and the improved capacitive performances for carbon-based supercapacitors, *J. Power Sources* 341 (2017) 448–456.
- [143] M.D. Stoller, S. Park, Y. Zhu, J. An, R.S. Ruoff, Graphene-based ultracapacitors, *Nano Lett.* 8 (2008) 3498–3502.
- [144] J. Wu, W. Pisula, K. Mullen, Graphenes as potential material for electronics, *Chem. Rev.* 107 (2007) 718–747.
- [145] V. Georgakilas, M. Otyepka, A.B. Bourlinos, V. Chandra, N. Kim, K.C. Kemp, P. Hobza, R. Zboril, K.S. Kim, Functionalization of graphene: covalent and non-covalent approaches, derivatives and applications, *Chem. Rev.* 112 (2012) 6156–6214.
- [146] G. Luo, L. Liu, J. Zhang, G. Li, B. Wang, J. Zhao, Hole defects and nitrogen doping in graphene: implication for supercapacitor applications, *ACS Appl. Mater. Interfaces* 5 (2013) 11184–11193.
- [147] Y. Li, Z. Zhou, P. Shen, Z. Chen, Spin gapless semiconductor-metal-half-metal properties in nitrogen-doped zigzag graphene nanoribbons, *ACS Nano* 3 (2009) 1952–1958.
- [148] K. Artyushkova, P. Atanassov, X-Ray Photoelectron spectroscopy for characterization of bio nano composite functional materials for energy harvesting technologies, *Chem. Phys. Chem.* 14 (2013) 2071–2080.
- [149] Y. Shao, S. Zhang, M.H. Engelhard, G. Li, G. Shao, Y. Wang, J. Liu, I.A. Aksay, Y. Lin, Nitrogen-doped graphene and its electrochemical applications, *J. Mater. Chem.* 20 (2010) 7491–7496.
- [150] J. Wang, B. Ding, Y. Xu, L. Shen, H. Dou, X. Zhang, Crumpled nitrogen-doped graphene for supercapacitors with high gravimetric and volumetric performances, *ACS Appl. Mater. Interfaces* 7 (2015) 22284–22291.
- [151] E. Haque, Md. M. Islam, E. Pourazadi, M. Hassan, S.N. Faisal, A.K. Roy, K. Konstantinov, A.T. Harris, A.I. Minett, V.G. Gomes, Nitrogen doped graphene via thermal treatment of composite solid precursors as a high performance supercapacitor, *RSC Adv.* 5 (2015) 30679–30686.
- [152] V. Chabot, F.M. Hassan, A. Yu, Nitrogen Doped Graphene as a high efficient electrode for next generation supercapacitor, *ECS Trans.* 50 (2013) 19–26.
- [153] D. Li, C. Yu, M. Wang, Y. Zhang, C. Pan, Synthesis of nitrogen doped graphene from graphene oxide within an ammonia flame for high performance supercapacitors, *RSC Adv.* 4 (2014) 55394–55399.
- [154] C. Li, Y. Hu, M. Yu, Z. Wang, W. Zhao, P. Liu, Y. Tong, X. Lu, Nitrogen doped graphene paper as a highly conductive, and light-weight substrate for flexible supercapacitors, *RSC Adv.* 4 (2014) 51878–51883.
- [155] L. Tang, Y. Yin, X. Yang, Y. Bo, H. Cao, W. Wang, I. Zhang, S. Bello, H. Lee, C. Cheng, Tunable band gaps and p-type transport properties of boron-doped graphenes by controllable ion doping using reactive microwave plasma, *ACS Nano* 6 (2012) 1970–1978.
- [156] R. Faccio, L. Fernandez-Werner, H. Pardo, C. Goyenola, O.N. Ventura, A.W. Mombru, Electronic and structural distortions in graphene induced by carbon vacancies and boron doping, *J. Phys. Chem. C* 114 (2010) 18961–18971.
- [157] J. Han, L.L. Zhang, S. Lee, J. Oh, K. Lee, J.R. Potts, J. Ji, X. Zhao, R.S. Ruoff, S. Park, Generation of B-doped graphene nanoplatelets using a solution process and their supercapacitor applications, *ACS Nano* 7 (2013) 19–26.
- [158] Z. Peng, R. Ye, J.A. Mann, D. Zakhidov, Y. Li, P.R. Malley, J. Lin, J.M. Tour, Flexible boron-doped laser induced graphene microsupercapacitors, *ACS Nano* 9 (2015) 5868–5875.
- [159] Y.S. Yun, H.H. Park, H. Jin, Pseudocapacitive effects of N-doped carbon nanotube electrodes in supercapacitor, *Materials* 5 (2012) 1258–1266.
- [160] A.R. John, P. Arumugam, Open ended nitrogen-doped carbon nanotubes for the electrochemical storage of energy in a supercapacitor electrode, *J. Power Sources* 277 (2015) 387–392.
- [161] D. Gueon, J.H. Moon, Nitrogen-doped carbon nanotube spherical particles for supercapacitor applications: emulsion-assisted compact packing and capacitance enhancement, *ACS Appl. Mater. Interfaces* 7 (2015) 20083–20089.
- [162] J. Patino, N. Salas, M. Gutierrez, D. Carriazo, M.L. Ferrer, F. Monte, Phosphorus-doped carbon-carbon nanotube hierarchical monoliths as true three-dimensional electrodes in supercapacitor cells, *J. Mater. Chem. A* 4 (2016) 1251–1263.
- [163] X. Li, S. Ding, X. Xiao, J. Shao, J. Wei, H. Pang, Y. Yu, N,S co-doped 3D mesoporous carbon- $\text{Co}_3\text{Si}_2\text{O}_5(\text{OH})_4$ architectures for high-performance flexible pseudo-solid-state supercapacitors, *J. Mater. Chem. A* 5 (2017) 12774–12781.

- [164] S. Saha, P. Samanta, N.C. Murmu, A. Banerjee, R.S. Ganesh, H. Inokawa, T. Kuila, Modified electrochemical charge storage properties of h-BN/rGO superlattice through the transition from n to p type semiconductor by fluorine doping, *Chem Ing J.* 339 (2018) 334–345.
- [165] S. Saha, M. Jana, P. Samanta, N.C. Murmu, T. Kuila, Efficient Access of voltammetric charge in hybrid supercapacitor configured with potassium incorporated nanographitic structure derived from cotton (*Gossypium arboreum*) as negative and Ni(OH)₂/rGO composite as positive electrode, *Ind. Eng. Chem. Res.* 55 (2016) 11074–11084.
- [166] Z. Zhian, L.Y. Qing, L. Jie, L.Y. Xiang, Effect of Ni-doping on electrochemical capacitance of MnO₂ electrode materials, *J. Cent. South Univ. Technol.* 5 (2007) 638–642.
- [167] K.K. Purushothaman, S. Vijayakumar, S. Nagamuthu, G. Muralidharan, Supercapacitor behaviour of cobalt-doped nickel oxide films, *Philos. Mag. Lett.* 92 (2012) 436–441.
- [168] E.L. Miller, R.E. Rocheleau, Electrochemical behavior of reactively sputtered iron-doped nickel oxide, *J. Electrochem. Soc.* 144 (1997) 3072–3077.
- [169] D. Han, X. Jing, J. Wang, P. Yang, D. Song, J. Liu, Porous lanthanum doped NiO microspheres for supercapacitor application, *J. Electroanal. Chem.* 682 (2012) 37–44.
- [170] K. Sathishkumar, N. Shanmugam, N. Kannadasan, S. Cholan, G. Viruthagiri, Synthesis and characterization of Cu²⁺ doped NiO electrode for supercapacitor application, *J. Sol-Gel Sci. Technol.* 74 (2015) 621–630.
- [171] D. Liang, S. Wu, J. Liu, Z. Tian, C. Liang, Co-doped Ni hydroxide and oxide nanosheet networks: laser-assisted synthesis, effective doping, and ultrahigh pseudocapacitor performance, *J. Mater. Chem. A* 4 (2016) 10609–10617.
- [172] J.W. Brown, P.S. Ramesh, D. Geetha, Fabrication of mesoporous iron (Fe) doped copper sulfide (CuS) nanocomposite in the presence of a cationic surfactant via mild hydrothermal method for supercapacitors, *Mater. Res. Exp.* 5 (2017) 2.
- [173] S. Repp, E. Harputlu, S. Gurgen, M. Castellano, N. Kremer, N. Pompe, J. Wörner, A. Hoffmann, R. Thomann, F.M. Emen, S. Weber, K. Ocakoglu, E. Erdem, Synergistic effects of Fe³⁺ doped spinel Li₄Ti₅O₁₂nanoparticles on reduced graphene oxide for high surface electrode hybrid supercapacitors, *Nanoscale* 10 (2018) 1877–1884.
- [174] F. Fusalba, N.E. Mehdi, L. Breau, D.I. Be'langer, Physicochemical and electrochemical characterization of polycyclopenta [2, 1-b;3, 4-b'] dithiophen-4-one as an active electrode for electrochemical supercapacitors, *Chem. Mater.* 11 (1999) 2743–2753.
- [175] K. Naoi, S. Suematsu, A. Manago, Electrochemistry of poly (1, 5-diaminoanthraquinone) and its application in electrochemical capacitor materials, *J. Electrochem. Soc.* 147 (2000) 420–426.
- [176] A. Clemente, S. Panero, E. Spila, B. Scrosati, Solid-state, polymer-based, redox capacitors, *Solid State Ionics* 85 (1996) 273–277.
- [177] K.S. Ryu, K.M. Kim, N.-G. Park, Y.J. Park, S.H. Chang, Symmetric redox supercapacitor with conducting polyaniline electrode, *J. Power Sources* 103 (2002) 305–309.
- [178] V.G. Phadnis, K.R. Jagdeo, Synthesis of Cd doped Polyaniline for supercapacitor, *Int. Refereed J. Eng. Sci.* 3 (2014) 9–13.
- [179] S.H. Kazemi, M.A. Kiani, R. Mohamadi, L. Eskandarian, Metal-polyaniline nanofibre composite for supercapacitor applications, *Bull. Mater. Sci.* 37 (2014) 1001–1006.
- [180] D.S. Patil, J.S. Shaikh, D.S. Dalavi, M.M. Karanjkar, R.S. Devan, Y.R. Ma, P.S. Patil, An Mn doped polyaniline electrode for electrochemical supercapacitor, *J. Electrochem. Soc.* 185 (2011) 1–5.
- [181] F. Jing, C. Mu, L. Hai, Z. Zhi-An, L. Yan-Qing, L. Jie, J. Cent, Hybrid supercapacitor based on polyaniline doped with lithium salt and activated carbon electrodes, *South Univ. Technol.* 16 (2009) 0434–0439.
- [182] B. He, Y. Zhou, W. Zhou, B. Dong, H. Li, Preparation and characterization of ruthenium-doped polypyrrole composites for supercapacitor, *Mater. Sci. Eng. A* 374 (2004) 322–326.
- [183] M.D. Ingram, H. Staesche, K.S. Ryder, 'Ladder-doped' polypyrrole: a possible electrode material for inclusion in electrochemical supercapacitors, *J. Power Sources* 129 (2004) 107–112.
- [184] Y. Huang, M. Zhu, Z. Pei, Y. Huang, H. Geng, C. Zhi, Extremely stable polypyrrole achieved via molecular ordering for highly flexible supercapacitors, *ACS Appl. Mater. Interfaces* 8 (2016) 2435–2440.
- [185] R. Ma, X. Liu, J. Liang, Y. Bando, T.i Sasaki, Molecular-scale heteroassembly of redoxable hydroxide nanosheets and conductive graphene into superlattice composites for high-performance supercapacitors, *Adv. Mater.* 26 (2014) 4173–4178.
- [186] J. Hu, G. Lei, Z. Lu, K. Liu, S. Sang, H. Liu, Alternating assembly of Ni-Al layered double hydroxide and graphene for high-rate alkaline battery cathode, *Chem. Commun.* 51 (2015) 9983–9986.
- [187] J. Li, Y. Yiliguma, G. Wang, Zheng, Carbon-coated nanoparticle superlattices for energy applications, *Nanoscale* 8 (2016) 14359–14368.
- [188] M. Shao, R. Zhang, Z. Li, M. Wei, D.G. Evans, X. Duan, Layered double hydroxides toward electrochemical energy storage and conversion: design, synthesis and applications, *Chem. Commun.* 51 (2015) 15880–15893.
- [189] J. Zhao, S. Xu, K. Tschulik, R.G. Compton, M. Wei, D. O'Hare, D.G. Evans, X. Duan, Molecular-scale hybridization of clay monolayers and conducting polymer for thin-film supercapacitors, *Adv. Funct. Mater.* 25 (2015) 2745–2753.
- [190] S. Saha, M. Jana, P. Khanra, P. Samanta, H. Koo, N.C. Murmu, T. Kuila, Band gap engineering of boron nitride by graphene and its application as positive electrode material in asymmetric supercapacitor device, *ACS Appl. Mater. Interfaces* 7 (2015) 14211–14222.
- [191] S. Saha, M. Jana, P. Samanta, N.C. Murmu, N.H. Kim, T. Kuila, J.H. Lee, Investigation of band structure and electrochemical properties of h-BN/rGO composites for asymmetric supercapacitor applications, *Mater. Chem. Phys.* 190 (2017) 153–165.
- [192] X. Ge, C. Gu, Z. Yin, X. Wang, J. Tu, J. Li, Periodic stacking of 2D charged sheets: self-assembled superlattice of Ni-Al layered double hydroxide (LDH) and reduced graphene oxide, *Nano Energy* 20 (2016) 185–193.
- [193] L. Zhang, H. Yao, Z. Li, P. Sun, F. Liu, C. Dong, J. Wang, Z. Li, M. Wu, C. Zhang, B. Zhao, Synthesis of delaminated layered double hydroxides and their assembly with graphene oxide for supercapacitor application, *J. Alloys Comp.* 711 (2017) 31–41.
- [194] M. Li, J.P. Cheng, J. Wang, F. Liu, X.B. Zhang, The growth of nickel-manganese and cobalt-manganese layered double hydroxides on reduced graphene oxide for supercapacitor, *Electrochim. Acta* 206 (2016) 108–115.
- [195] P. Fernandez, M. Bissett, H. Ago, Synthesis, structure and applications of graphene-based 2D heterostructures, *Chem. Soc. Rev.* 46 (2017) 4572–4613.